Journal of Theoretical Biology 483 (2019) 110001

Contents lists available at ScienceDirect

Journal of Theoretical Biology

journal homepage: www.elsevier.com/locate/jtb

# Coevolution of cannibalistic predators and timid prey: evolutionary cycling and branching

Sami O. Lehtinen*, Stefan A.H. Geritz

*Department of Mathematics and Statistics, University of Helsinki, FIN-00014, Finland*

ARTICLE INFO

*Article history:*
Received 25 July 2019
Revised 4 September 2019
Accepted 6 September 2019
Available online 7 September 2019

*Keywords:*
Adaptive dynamics
Critical function analysis
Delayed evolutionary branching
Ecological bistability
Fold bifurcation of periodic orbits
Hopf bifurcation

ABSTRACT

We investigate the coevolution of cannibalistic predators and timid prey, which seek refuge upon detecting a predator. To understand how the species affect each other's evolution, we derived the ecological model from individual-level processes using ordinary differential equations. The ecological dynamics exhibit bistability between equilibrium and periodic attractors, which may disappear through catastrophic bifurcations. Using the critical function analysis of adaptive dynamics, we classify general trade-offs between cannibalism and prey capture that produce different evolutionary outcomes. The evolutionary analysis reveals several ways in which cannibalism emerges as a response to timidity of the prey. The long-term coevolution either attains a singularity, or becomes cyclic through two mechanisms: genetical cycles through Hopf bifurcation of the singularity, or ecogenetical cycles involving abrupt switching between ecological attractors. Further diversification of cannibalism occurs through evolutionary branching, which is predicted to be delayed when simultaneous prey evolution is necessary for the singularity's attainability. We conclude that predator-prey coevolution produces a variety of outcomes, in which evolutionary cycles are commonplace.



## 1. Introduction

Predators constitute a major cause of prey death, whereupon the prey are under strong selection to adopt better methods for detecting, avoiding, or fending off predators. At the same time, the predators are forced to improve their skills at tracking and killing the prey, or to seek an alternative food source such as cannibalising their young. Cannibalism has been recorded in a wide range of predator species, especially among fish and insects (Fox 1975; Polis 1981). It is thus only natural that the evolution of the prey influences that of the predator, and vice versa (Abrams 2000). Dawkins and Kreb's (1979) analogy of an evolutionary arms race illustrates the idea behind such coevolving interactions, in which both species adapt to each other in a continual struggle for existence. Such adaptations have been observed in various predator-prey relationships, including spiders and bees (Heiling and Herberstein 2004), snakes and lizards (Downes and Shine 1998), and crabs and snails (West et al. 1991). Understanding the evolution of predator-prey interactions helps to understand the function of their behaviour.

Predator-prey coevolution has motivated a variety of theoretical models, revealing intriguing long-term evolutionary implications. Of particular interest has been the question of whether long-term coevolution would eventually come to a stasis, such as an evolutionary uninvadable trait (ESS; Maynard Smith and Price 1973; Rosenzweig 1973; Brown and Vincent 1992), or continue indefinitely in accordance with the Red Queen hypothesis (Van Valen 1973). Abrams (1986) showed that the arms race analogy for runaway selection fails when investments in predation related adaptations are traded off with other life-history traits. Later models revealed that predator-prey coevolution often produces long-term cycles in phenotypic traits, which can be driven by different mechanisms (Marrow et al. 1992; Dieckmann et al. 1995; Khibnik and Kondrashov 1997; Kisdi et al. 2001; Dercole et al. 2003). These include genetically and ecogenetically driven cycles, where the latter may involve abrupt switching between alternative ecological attractors. Kisdi et al. (2001) and Dercole (2003) further demonstrated how such cycles can be driven by a recurrent evolutionary branching and extinction process. Along any such an evolutionary cycle, investments in predation-related traits fluctuate. While models with evolutionary cycles typically assume equilibrium ecological dynamics, Abrams and Matsuda (1997)

* Corresponding author.
*E-mail address:* sami.lehtinen@helsinki.fi (S.O. Lehtinen).

https://doi.org/10.1016/j.jtbi.2019.110001

demonstrated that ecological dynamics can also become cyclic as a consequence of predator-prey coevolution.

There are several shortcomings with previous modelling approaches. They most often lack derivation from individual-level processes, making it difficult to investigate how evolution affects the behaviour of predator and prey individuals. It is often unclear when adaptation to predation by one species is an evolutionary response to other species, since other ecological factors can influence such adaptations as well (Abrams 1990). These include apparent competition between two prey species that share a common predator (Holt 1977; Abrams and Matsuda 1993). Another common shortcoming concerns the trade-off relationships of adaptations. In nature, investments in predation-related traits are typically traded off with other behavioural characteristics, such as the foraging efficiency of prey individuals (Lima and Dill 1990). Previous models often assume a particular shape of such trade-off functions, but in reality the shape is uncertain and cumbersome to obtain empirically (Kisdi 2006). The assumed shapes remain the least justified element of the models.

How can one explain cannibalism as an adaptation to predation? When prey availability is limited, cannibalism may emerge and represent a 'life boat mechanism' that saves a predator population from going extinct (van den Bosch et al. 1988; Getto et al. 2005). However, previous theoretical models neglect the possible influence of simultaneous prey evolution. Moreover, empirical work suggest that cannibalism is sometimes favourable even when their typical food is abundant (Fox 1975, pp. 90–91; Stenseth 1985). The rate of cannibalism also varies greatly between species, contributing less than 1% of diet in the dragonfly *Pyrrhosoma nymphula* (Lawton 1970), whereas in the wolf spider *Lycosa lugubris* it is 16% (Edgar 1969). In some ecological environments, populations of the perch *Perca fluviatilis* can sustain solely on cannibalism (Popova and Sytina 1977). In addition to the nutritional value, cannibalism is an effective way of eliminating competitors for resources or sexual partners (Hrdy 1979; Claessen et al. 2000). There is unlikely any single explanation for cannibalism, although predation may promote such behaviour.

This study investigates the emergence of cannibalism and the long-term implications of predator-prey coevolution. We derive the ecological model from individual-level processes as in Lehtinen and Geritz (2019) with timid prey and cannibalistic predators. The prey are characterised by their readiness to seek refuge upon detecting a predator, and where the predators cannibalise on their conspecific young. While Lehtinen and Geritz (2019) focused on the evolution of timidity of the prey with a fixed rate of cannibalism, here cannibalism is also considered as an evolving trait. Using the critical function analysis of adaptive dynamics (de Mazancourt and Dieckmann 2004; Bowers et al. 2005; Kisdi 2006), we treat a general class of trade-offs between cannibalism and prey capture. We conduct an explorative analysis to the extent to which trade-off properties are associated with different evolutionary outcomes. These include investigation into the emergence of cannibalism, and how it is affected by prey evolution. The long-term coevolutionary outcomes include cyclic Red Queen dynamics and further diversification of cannibalism through evolutionary branching. Our analysis is characterised by an emphasis on capturing only the most essential model ingredients, and on making minimal assumptions about the shape of the trade-off.

The organisation of the paper is as follows. We begin in Section 2 by setting the ecological stage on which evolution takes place. This stage setting is important because evolution by natural selection is driven by individual-level processes, which form the basis for the ecological environment. We proceed in Section 3 by establishing the tools that will be used in the evolutionary analysis. Then, in Section 4 we investigate the coevolution of cannibalistic predators and timid prey, with corresponding subsections for the emergence of cannibalism, evolutionary branching, and evolutionary cycling. Finally, the implications of our findings are discussed in Section 5.

## 2. Ecological setting

### 2.1. Model ingredients

Consider an ecological environment consisting of a single prey and predator species. The prey are characterised by their timidity, that is, their readiness to seek and remain in refuge after detecting an adult predator. The predators are divided into adults and juveniles, where the adults are characterised by their cannibalistic tendencies towards the juveniles, and only the adults capture the prey. Within the prey and the predator species, many different types may coexist that differ in these characteristic features. We now derive the ecological model assuming the same individual-level processes as in Lehtinen and Geritz (2019), who considered only a single predator type. Frequently used symbols are found in Table 1.

Assume that each prey individual of a population $x_i$ detects a predator and moves to refuge at rate $b_i$, and has the mean sojourn time $\tau_i$ in refuge. The product, $b_i\tau_i$, represents the level of timidity of the prey. In the absence of timidity, $b_i\tau_i = 0$, the prey make no use of the refuge. Biologically, 'refuge' can be interpreted as a physical place, such as a tree, or a state of being vigilant. While a prey is in refuge, it gains protection from predation but has halted foraging. As in Lehtinen and Geritz (2019), we assume that prey react only to adult predators, but they are unable to distinguish searching predators from those that are handling. Throughout this paper, an unspecified 'predator' always refers to an adult individual. We divide each prey population $x_i$ into foragers $x_i^F$ and hiders $x_i^H$,

$$x_i = x_i^F + x_i^H. \tag{1}$$

All prey individuals have the same natural death rate $\mu$, which is independent of the prey and the predator populations. The foraging prey compete for some common resource so that the per capita birth rate, $G(\sum_j x_j^F)$, is limited by their total population. We assume that $G$ decreases monotonically and that there exists $x_0$ such that $G(x_0) = \mu$. In the absence of predators, the prey populations attain the equilibrium state $x_0$, which is the prey's carrying capacity. Examples of mechanistic derivations of the birth rate $G$ based on competition for breeding sites or food are found in Geritz and Gyllenberg (2014). For the numerical analysis, we choose $G(\sum_j x_j^F) = a - c\sum_j x_j^F$ when $\sum_j x_j^F < a/c$, otherwise it is zero.

**Table 1**
List of model parameters (Lehtinen and Geritz 2019).

| **Prey parameters** | |
|---|---|
| Symbol | Description |
| $b$ | Rate of moving to refuge |
| $\tau$ | Mean sojourn time in refuge |
| $\mu$ | Natural death rate |
| $G$ | Birth rate (function of foraging prey) |
| **Predator parameters** | |
| Symbol | Description |
| $\alpha$ | Rate of cannibalism |
| $\beta(\alpha)$ | Rate of prey capture |
| $h$ | Handling time per captured prey |
| $\gamma$ | Conversion efficiency of prey capture |
| $\lambda$ | Conversion efficiency of cannibalism |
| $T$ | Mean maturation time |
| $\delta$ | Adult death rate |
| $\sigma$ | Juvenile death rate |

As for the predators, we assume that each adult predator individual of a population $y_j$ cannibalises on the conspecific juveniles at the rate $\alpha_j$. All predator types share the same average conversion efficiency $\lambda$ of cannibalism into reproduction of new juveniles. The prey are captured at the rate $\beta$, with the conversion efficiency $\gamma$. The predators have the mean handling time $h$ per prey capture, while the handling time of cannibalism is assumed to be negligible. Moreover, feeding on the prey is more beneficial than cannibalism, hence $\lambda < \gamma$. Biologically, these assumptions imply that the victims of cannibalism are smaller or otherwise easier to digest and kill than the typical prey, and are supported by a plethora of observed examples (Fox 1975; Polis 1981). Finally, the adult and juvenile predators have the natural death rates $\delta$ and $\sigma$, respectively. We divide each predator population $y_j$ into searchers $y_j^S$ and handlers $y_j^H$,

$$y_j = y_j^S + y_j^H, \tag{2}$$

and the predators produce juveniles of the same type, which have the population $z_j$.

To extend the model of Lehtinen and Geritz (2019), we further assume a trade-off relationship between prey capture and cannibalism. The trade-off is described by the nonnegative and decreasing function $\beta(\alpha)$. We abstain from choosing any specific shape for the trade-off, assuming only that adaptation to cannibalism results in decreased prey capture success. For instance, large jaws help to capture and kill large prey individuals. At the same time, such jaws are likely inconvenient when cannibalising on small eggs or post-hatching stages.

### 2.2. Timescale separation

The ecological dynamics of all individual-level processes are described by a system of differential equations, one for each individual-state. In the simplest case with only a single predator and prey type present, the system consists of five differential equations. To ease the qualitative analysis, we divide the ecological interactions into separate timescales based on their occurrences. In particular, we assume a short timescale for the interactions between foraging and hiding prey states, and between searching and handling predator states; an intermediate timescale for the birth and death of juvenile predators; and a long timescale for juvenile maturation and rest of the birth and death terms. This separation of timescales is the same as in Lehtinen and Geritz (2019). Appendix A provides the full system of the ecological dynamics and the technical details on timescale separation.

The short timescale dynamics is described by

$$\dot{x}_i^F = -b_i x_i^F \sum_{j'} y_{j'} + \frac{1}{\tau_i} x_i^H, \tag{3}$$

$$\dot{y}_j^S = -\beta(\alpha_j) y_j^S \sum_{i'} x_{i'}^F + \frac{1}{h} y_j^H, \tag{4}$$

which have the unique quasi-steady state,

$$x_i^F = \frac{x_i}{1 + b_i \tau_i \sum_{j'} y_{j'}}, \tag{5}$$

$$y_j^S = \frac{y_j}{1 + \beta(\alpha_j) h \sum_{i'} x_{i'}^F}. \tag{6}$$

The parameters $b_i$ and $\tau_i$ of the prey type $i$ are now always found in the product $b_i\tau_i$, which describes the level of timidity of the prey (Geritz and Gyllenberg 2014; Lehtinen and Geritz 2019). For convenience, we treat this product as a single parameter, $b\tau_i$.

Next, assuming that $x_i^F$ and $y_j^S$ have attained their respective quasi-steady states, the intermediate timescale dynamics of the juvenile predators is described by

$$\dot{z}_j = \gamma \beta(\alpha_j) y_j^S \sum_{i'} x_{i'}^F + \lambda \alpha_j y_j^S \sum_{j'} z_{j'} - z_j \sum_{j'} \alpha_{j'} y_{j'}^S - \sigma z_j. \tag{7}$$

A biological restriction on the efficiency on cannibalism is $\lambda < 1$, that is, on average less than one new juvenile is produced from a cannibalistic capture. Observe that the total juvenile predator population is given by

$$\sum_{j'} z_{j'} = \frac{\gamma \sum_{i'} x_{i'}^F \sum_{j'} \beta(\alpha_{j'}) y_{j'}^S}{\sigma + (1-\lambda) \sum_{j'} \alpha_{j'} y_{j'}^S}. \tag{8}$$

By using the above equation, it follows that the juvenile predator population of type $j$ has the unique quasi-steady state

$$z_j = \frac{\gamma y_j^S \sum_{i'} x_{i'}^F}{\sigma + \sum_{j'} \alpha_{j'} y_{j'}^S} \left( \beta(\alpha_j) + \frac{\alpha_j \lambda \sum_{j'} \beta(\alpha_{j'}) y_{j'}^S}{\sigma + (1-\lambda) \sum_{j'} \alpha_{j'} y_{j'}^S} \right). \tag{9}$$

Finally, assuming that $z_j$ has attained the above quasi-steady state, the long timescale dynamics is described by

$$\dot{x}_i = x_i^F G\Big( \sum_{i'} x_{i'}^F \Big) - \mu x_i - x_i^F \sum_{j'} \beta(\alpha_{j'}) y_{j'}^S, \tag{10}$$

$$\dot{y}_j = \frac{1}{T} z_j - \delta y_j. \tag{11}$$

Recall that $T$ describes the mean maturation time of juveniles predators, and $\delta$ is the death rate of the adults.

### 2.3. Functional response

The functional response $F_{ij}(x, y)$ of the predator type $j$ for the prey type $i$ is equal to the rate $\beta(\alpha_j) x_i^F y_j^S$ of prey capture divided by the predator population $y_j$,

$$F_{ij}(x, y) = \frac{\beta(\alpha_j) x_i^F}{1 + \beta(\alpha_j) h \sum_{i'} x_{i'}^F}, \tag{12}$$

which is the DeAngelis-Beddington functional response with multiple prey and predator types (DeAngelis et al. 1975; Beddington 1975; Geritz and Gyllenberg 2012). Here, $x$ and $y$ are the population vectors that comprise all prey and predator types present. Recall that the quasi-steady states for the foraging prey $x_i^F$ and juvenile predators $z_j$ depend on $x$ and $y$, as described by (5) and (9). Similarly, the functional response $C_{kj}(x, y)$ of the predator type $j$ for the juvenile predator type $k$ is equal to the rate $\alpha_j z_k y_j^S$ of cannibalism divided by the predator population $y_j$,

$$C_{kj}(x, y) = \frac{\alpha_j z_k}{1 + \beta(\alpha_j) h \sum_{i'} x_{i'}^F}. \tag{13}$$

Now, by using the above functional responses, we can write the long timescale dynamics as

$$\dot{x}_i = x_i^F G\left( \sum_{i'} x_{i'}^F \right) - \mu x_i - \sum_{j'} F_{ij'}(x, y) y_{j'}, \tag{14}$$

$$\dot{y}_j = \left( \gamma \sum_{i'} F_{i'j}(x, y) + \lambda \sum_{j'} C_{j'j}(x, y) \right) A(x, y) y_j - \delta y_j, \tag{15}$$

and where

$$A(x, y) = \frac{1}{T\left( \sigma + \sum_{j'} \alpha_{j'} y_{j'}^S \right)}. \tag{16}$$

Since the model was derived from individual-level processes, all terms in the above equations have clear-cut and biologically sound interpretations. The term $\gamma \sum_{i'} F_{i'j}(x, y)$ describes the rate at which juveniles are produced per unit of time by the predator type $j$ through prey capture. Similarly, juvenile production through cannibalism is described by the term $\lambda \sum_{j'} C_{j'j}(x, y)$. But since all juveniles are equally under the threat of cannibalism during their juvenile period, and they may die to natural causes as well, only some reach maturity. The recruitment rate into the adult population is thus described by the term (16). In the absence of cannibalism, $\alpha = 0$, we recover the model by Geritz and Gyllenberg (2014), and in the absence of both cannibalism and timidity, $\alpha = b\tau = 0$, we recover the classical Rosenzweig-MacArthur (1963) model.

### 2.4. Monomorphic predator-prey populations

The population dynamics of a single prey and predator type can be written as

$$\dot{x} = x^F G\left(x^F\right) - \mu x - \frac{\beta(\alpha) x^F y}{1 + \beta(\alpha) h x^F}, \tag{17}$$

$$\dot{y} = \frac{\gamma}{T} \frac{\beta(\alpha) x^F y}{\sigma(1 + \beta(\alpha) h x^F) + (1 - \lambda)\alpha y} - \delta y, \tag{18}$$

where $x^F = x/(1 + b\tau y)$. The above equations are almost the same as in Lehtinen and Geritz (2019), where $\beta(\alpha)$ was a fixed constant. However, many of the results obtained by Lehtinen and Geritz are present also for a trade-off function $\beta(\alpha)$. Recall that in the absence of predators, the prey attains the equilibrium state $x_0$. The predator invades the prey-only environment $x_0$ if and only if

$$\beta(\alpha) > \frac{\delta\sigma T}{x_0(\gamma - \delta\sigma h T)} \qquad \text{and} \qquad \gamma > \delta\sigma h T. \tag{19}$$

Whenever the above conditions are satisfied, there exists a unique interior equilibrium $(\bar{x}, \bar{y})$. This equilibrium can switch stability through subcritical or supercritical Hopf bifurcation. A detailed analysis of the ecological dynamics described by (17) and (18) for a constant $\beta(\alpha)$ is found in Lehtinen and Geritz (2019). In particular, they classified four qualitative different bifurcation regions, and demonstrated that the ecological dynamics can exhibit bistability between equilibrium and periodic attractors, as caused by subcritical Hopf and fold bifurcation of periodic orbits. Fig. 1 provides an example of ecological bistability between equilibrium and periodic attractors of (17) and (18).

Subcritical Hopf bifurcation generates ecological bistability by stabilising an equilibrium while a periodic attractor is already present. As a side product, subcritical Hopf yields an unstable periodic orbit that separates the regions of attraction between equilibrium and periodic attractors. Fold bifurcation of periodic orbits causes bistability to disappear as the stable periodic attractor collides with the unstable orbit. This kind of bifurcation pattern occurs when the parameters $b\tau$ and $\alpha$ vary. However, a positive $\alpha$ value is necessary for ecological bistability. It is typically present for the parameter values between the two catastrophic bifurcation points, but sometimes only the fold bifurcation is observed for positive values of $b\tau$. Here, we found that the occurrence of ecological bistability is largely independent of the specific form of the trade-off function $\beta(\alpha)$, as long as $\beta(0)$ is sufficiently large.

The numerical analysis was done using the *Mathematica*® software, as in Lehtinen and Geritz (2019). Periodic attractors were found by numerically integrating (17) and (18) using an explicit Runge-Kutta method for *NDSolve* and with the initial condition $(x, y) = (x_0, 0.001)$. Then, together with the *EventLocator* method, convergence to the attractor was evaluated using a Poincaré section. We collected data of the solution curve until the distance between two consecutive equilibrium points of a Poincaré map was smaller than $10^{-5}$, after which we discarded the transient data. Whenever there exists bistability, the unstable periodic orbit was found using the same method, but for reverse direction and by setting the initial value in the interior of the stable periodic attractor.

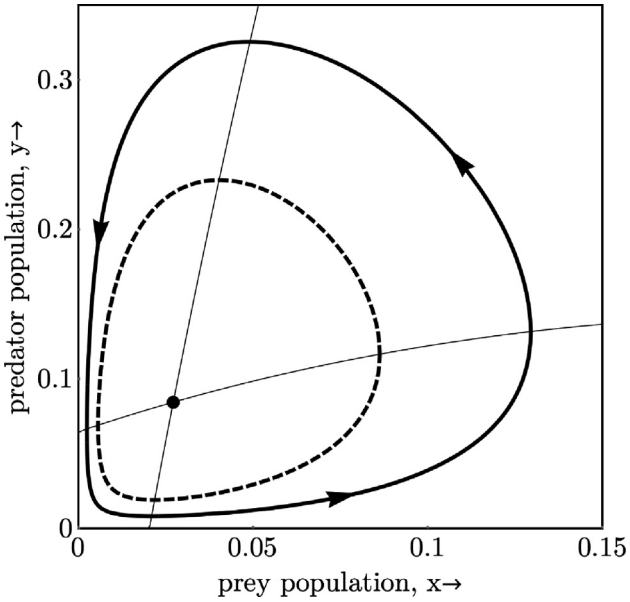


**Fig. 1.** Ecological bistability between equilibrium and periodic attractors (Lehtinen and Geritz 2019). Thin lines indicate isoclines of the ecological dynamics, and the dashed curve indicates the unstable periodic orbit that separates the regions of attraction. In this figure, the prey and predator traits have the values $b\tau = 0.44$, $\alpha = 6$, and $\beta(6) = 15$, and other model parameters have the values $c = 2$, $a = 2$, $\mu = 1$, $\gamma = 3$, $\lambda = 0.6$, $\delta = 1$, $h = 1$, $T = 1$, and $\sigma = 0.7$.

## 3. Adaptive dynamics

### 3.1. Evolutionary setting

The coevolution between the predator and its prey is investigated using the framework of adaptive dynamics (Geritz et al. 1998). The evolving traits considered in this study are timidity of the prey and cannibalism of the predator. Recall that the level of timidity is described by the product $b\tau$, while the rate at which the predator cannibalises the conspecific juveniles is described by $\alpha$. Cannibalism is traded off with prey capture, described by an arbitrary nonnegative function $\beta(\alpha)$ satisfying $\beta'(\alpha) < 0$. The resident trait values $b\tau$ and $\alpha$ change gradually through repeated invasions and replacements by successful mutants. The long-term trait dynamics take place on an evolutionary timescale that is considerably longer than the ecological timescale. As is typical in adaptive dynamics, we assume that mutations have small phenotypic effects, and are sufficiently infrequent that the resident environment has attained an attractor before a mutant appears.

The ecological environment set by the resident traits determines whether a novel mutant type has a positive probability of invasion. In many cases when a mutant appears with a positive invasion probability, the mutant dies out due to demographic stochasticity. But since the environment remains at the same ecological attractor, eventually a mutant appears that successfully invades the resident environment. If such an invasion would be impossible if the roles were switched, the mutant replaces the resident and establishes the new resident environment.

The Tube Theorem of adaptive dynamics (Geritz et al. 2002) ensures that the new resident type settles on an environment that is generally arbitrarily close to the previous resident environment.

Thus, through small evolutionary steps, the resident environment tends to track the same branch of ecological attractors. Abrupt changes in the resident environments can occur only when the current branch of ecological attractors vanishes through a catastrophic bifurcation. Therefore, if a successful invasion and replacement event causes a catastrophic bifurcation of the ecological attractor, the new resident either settles on an alternative attractor or goes extinct. In our model, abrupt switching to an alternative attractor is possible because of subcritical Hopf and fold bifurcations, while evolutionary extinction is impossible when single prey and predator types are present (Lehtinen and Geritz 2019). Whenever the equilibrium attractor undergoes subcritical Hopf bifurcation, it disappears and the ecological environment shifts to the periodic attractor. A fold bifurcation causes a similar shift from periodic to equilibrium environment. Note that whenever the environment has undergone such an attractor switch, the direction of evolution may change as well (Dercole and Rinaldi 2002; Lehtinen and Geritz 2019).

For the evolutionary analysis, it is helpful to write the ecological dynamics in terms of the resident environment $E$. Then, the dynamics (14) and (15) are equivalent with

$$\dot{x}_i = f(b\tau_i, E)x_i, \tag{20}$$

$$\dot{y}_j = g(\alpha_j, \beta(\alpha_j), E)y_j, \tag{21}$$

where the environment $E = (E_1, E_2, E_3, E_4)$ is defined by

$$\begin{aligned} E_1 &= \sum_{j'} y_{j'} && \text{(Predator population)} \\ E_2 &= \sum_{i'} \frac{x_{i'}}{1 + b\tau_{i'}E_1} && \text{(Foraging prey population)} \\ E_3 &= \sum_{j'} \frac{\beta(\alpha_{j'})y_{j'}}{1 + \beta(\alpha_{j'})hE_2} && \text{(Predation pressure)} \\ E_4 &= \sum_{j'} \frac{\alpha_{j'}y_{j'}}{1 + \beta(\alpha_{j'})hE_2} && \text{(Cannibalistic pressure)} \end{aligned} \tag{22}$$

and where the instantaneous per capita population growth rates $f$ and $g$ are given by

$$f(b\tau_i, E) = \frac{G(E_2) - E_3}{1 + b\tau_i E_1} - \mu, \tag{23}$$

$$\begin{aligned} g(\alpha_j, \beta(\alpha_j), E) = {} & \frac{\gamma}{T(\sigma + E_4)} \frac{E_2}{1 + \beta(\alpha_j)hE_2} \\ & \times \left( \beta(\alpha_j) + \frac{\alpha_j \lambda E_3}{\sigma + (1 - \lambda)E_4} \right) - \delta. \end{aligned} \tag{24}$$

Consider a resident environment $E$ set by a single prey type $b\tau$ and a single predator type $\alpha$. The fitness of a mutant prey or predator type is determined by its average growth rate in the resident environment. A positive fitness implies positive probability of invasion, otherwise invasion is impossible. When the environment is at a periodic attractor, with the period $t_p = t_p(b\tau, \alpha, \beta(\alpha))$, the fitness of a mutant prey type $b\tau_m$ is described by

$$r(b\tau_m, b\tau, \alpha, \beta(\alpha)) = \frac{1}{t_p} \int_0^{t_p} f(b\tau_m, E(t))dt, \tag{25}$$

and similarly, the fitness of a mutant predator type $\alpha_m$ is described by

$$s(\alpha_m, \beta(\alpha_m), b\tau, \alpha, \beta(\alpha)) = \frac{1}{t_p} \int_0^{t_p} g(\alpha_m, \beta(\alpha_m), E(t))dt. \tag{26}$$

When the environment $E$ is at an equilibrium attractor, the growth rates $f$ and $g$ fully determine the invasion fitnesses, and there is no need to take the time-average. For periodic attractors, the values of the invasion fitnesses were found numerically using *NIntegrate* method of *Mathematica*® from $t = 0$ to $t = t_p$, as in Lehtinen and Geritz (2019).

By definition, every resident must have fitness equal to zero, as on average, their abundances neither grow nor decline. Thus, the resident $b\tau$ and $\alpha$ satisfy $r(b\tau, b\tau, \alpha, \beta(\alpha)) = s(\alpha, \beta(\alpha), b\tau, \alpha, \beta(\alpha)) = 0$. As the environment $E$ consists of four components, then generally at most four prey and predator types can coexist; a result known as the competitive exclusion principle (MacArthur and Levins 1964; Geritz et al. 1997). Thus, the environment sets the limit to the maximum diversity attainable through the process of evolutionary branching. Note that while it is possible to find parameters such that four species types coexist on the ecological timescale, such coexistence may perish through long-term evolution.

### 3.2. Evolutionary dynamics

The directions of prey and predator evolution are described by the signs of the fitness derivatives with respect to the mutants and evaluated for the resident type. This means that the sign of $[\partial r/\partial b\tau_m]_{b\tau_m = b\tau}$ describes whether evolution of the prey favours higher or lower levels of timidity, and similarly for the evolution of cannibalism of the predator. The rate and direction of long-term evolution is predicted by the canonical equation of adaptive dynamics (Dieckmann and Law 1996; Champagnat et al. 2001),

$$\begin{aligned} \dot{b\tau} &= C(b\tau, \alpha, \beta(\alpha)) \left[ \frac{\partial r(b\tau_m, b\tau, \alpha, \beta(\alpha))}{\partial b\tau_m} \right]_{b\tau_m = b\tau}, \\ \dot{\alpha} &= D(b\tau, \alpha, \beta(\alpha)) \left[ \frac{\partial s(\alpha_m, \beta(\alpha_m), b\tau, \alpha, \beta(\alpha))}{\partial \alpha_m} \right]_{\alpha_m = \alpha}. \end{aligned} \tag{27}$$

Here, the nonnegative coefficients $C$ and $D$ govern the relative speeds of prey and predator evolution, which incorporate variation in the occurrence of mutations and the mutant trait distributions. These coefficients generally depend on the resident trait values and the ecological environment. In this study, the aim is to investigate different evolutionary outcomes by making minimal assumptions about the explicit forms of $C$ and $D$, as they are difficult to obtain in periodic environments. For convenience, we assume that the coefficients $C$ and $D$ are differentiable, so that we can later calculate the Jacobian matrix of the canonical equation.

Coevolutionary singularity is a point at which directional evolution vanishes for both species. In other words, coevolutionary singularity is a trait pair $(b\tau^*, \alpha^*)$ at which

$$\left[ \frac{\partial r}{\partial b\tau_m} \right]_{\substack{b\tau_m = b\tau = b\tau^* \\ \alpha = \alpha^*}} = 0, \tag{28}$$

and

$$\left[ \frac{\partial s}{\partial \alpha_m} \right]_{\substack{b\tau = b\tau^* \\ \alpha_m = \alpha = \alpha^*}} = s_1 + \beta'(\alpha^*)s_2 = 0. \tag{29}$$

Here, the terms $s_1$ and $s_2$ are the partial derivatives of the predator's invasion fitness function $s$, which are then evaluated at the singularity.

In addition to coevolutionary singularity, we define a boundary attractor to be a pair of strategies at which one of the trait values equals to zero, whereas the other trait value is positive and for which the fitness derivative vanishes. This means that the trait pair $(b\tau_0^*, 0)$ is a boundary attractor if

$$\left[ \frac{\partial r}{\partial b\tau_m} \right]_{\substack{b\tau_m = b\tau = b\tau_0^* \\ \alpha = 0}} = 0, \tag{30}$$

$$\left[ \frac{\partial s}{\partial \alpha_m} \right]_{\substack{b\tau = b\tau_0^* \\ \alpha_m = \alpha = 0}} < 0, \tag{31}$$

and similarly, the trait pair $(0, \alpha_0^*)$ is a boundary attractor if

$$\left[\frac{\partial r}{\partial b\tau_m}\right]_{\substack{b\tau_m=b\tau=0\\ \alpha=\alpha_0^*}} < 0, \tag{32}$$

$$\left[\frac{\partial s}{\partial \alpha_m}\right]_{\substack{b\tau=0\\ \alpha_m=\alpha=\alpha_0^*}} = 0. \tag{33}$$

When no nearby mutants of either the prey or the predator species can invade a singularity, it is evolutionary uninvadable. In the literature, such singularities are often called evolutionary stable (ESS, Maynard Smith 1982). However, this term can easily cause unwanted confusion. Evolutionary stability gives no information whether it is attainable through evolution, and vice versa, a singularity can be attainable but lack evolutionary stability. To avoid confusion, we shall avoid using the term evolutionary stability.

Since only one mutant type can be present at any time, then at evolutionary uninvadable singularity both of the invasion fitness functions are at local maximum, that is,

$$\mathscr{E}_1 = \left[\frac{\partial^2 r}{\partial b\tau_m^2}\right]_{\substack{b\tau_m=b\tau=b\tau^*\\ \alpha=\alpha^*}} \tag{34}$$

and

$$\begin{aligned}\mathscr{E}_2 &= \left[\frac{\partial^2 s}{\partial \alpha_m^2}\right]_{\substack{b\tau=b\tau^*\\ \alpha_m=\alpha=\alpha^*}}\\ &= s_2\beta''(\alpha^*) + s_{22}\beta'(\alpha^*)^2 + 2s_{12}\beta'(\alpha^*) + s_{11}\end{aligned} \tag{35}$$

are both negative. This concept is easily applicable to the boundary attractors: $(b\tau_0^*, 0)$ is uninvadable when $\mathscr{E}_1 < 0$, and similarly, $(0, \alpha_0^*)$ is uninvadable when $\mathscr{E}_2 < 0$.

### 3.3. Convergence stability

A coevolutionary singularity is convergence stable when it is locally attainable through evolution (Dieckmann and Law 1996; Marrow et al. 1996; Leimar 2009). The coevolutionary dynamics typically depend on the relative speeds of prey and predator evolution, and so the concept of convergence stability is considerably more complicated than in single species evolution. A coevolutionary singularity is locally attainable when all eigenvalues of the Jacobian matrix of the canonical equation have negative real parts. The entries of the $2\times 2$ Jacobian matrix $J$ of (27) evaluated at $(b\tau^*, \alpha^*)$ are given by

$$J_{11} = C\cdot\frac{\partial}{\partial b\tau}\left[\frac{\partial r}{\partial b\tau_m}\Big|_{b\tau_m=b\tau}\right]_{\substack{b\tau=b\tau^*\\ \alpha=\alpha^*}} = C\cdot(\mathscr{E}_1+\mathscr{M}_1), \tag{36}$$

$$J_{12} = C\cdot\frac{\partial}{\partial \alpha}\left[\frac{\partial r}{\partial b\tau_m}\Big|_{b\tau_m=b\tau}\right]_{\substack{b\tau=b\tau^*\\ \alpha=\alpha^*}} = C\cdot\mathscr{A}_1, \tag{37}$$

$$J_{21} = D\cdot\frac{\partial}{\partial b\tau}\left[\frac{\partial s}{\partial \alpha_m}\Big|_{\alpha_m=\alpha}\right]_{\substack{b\tau=b\tau^*\\ \alpha=\alpha^*}} = D\cdot\mathscr{A}_2, \tag{38}$$

$$J_{22} = D\cdot\frac{\partial}{\partial \alpha}\left[\frac{\partial s}{\partial \alpha_m}\Big|_{\alpha_m=\alpha}\right]_{\substack{b\tau=b\tau^*\\ \alpha=\alpha^*}} = D\cdot(\mathscr{E}_2+\mathscr{M}_2), \tag{39}$$

and where

$$\mathscr{M}_1 = \left[\frac{\partial^2 r}{\partial b\tau\,\partial b\tau_m}\right]_{\substack{b\tau_m=b\tau=b\tau^*\\ \alpha=\alpha^*}}, \tag{40}$$

$$\mathscr{M}_2 = \left[\frac{\partial^2 s}{\partial \alpha\,\partial \alpha_m}\right]_{\substack{b\tau=b\tau^*\\ \alpha_m=\alpha=\alpha^*}}. \tag{41}$$

By the Routh-Hurwitz criteria, the singularity is convergence stable if and only if $\det J > 0$ and $\operatorname{tr} J < 0$. Based on the dependence on the positive coefficients $C$ and $D$, we can classify two different types of convergence stability.

A coevolutionary singularity is *strongly convergence stable* when it is locally attainable for all coefficients $C$ and $D$. This means that the following inequality must hold for $\det J$ to be positive,

$$(\mathscr{E}_1+\mathscr{M}_1)(\mathscr{E}_2+\mathscr{M}_2) > \mathscr{A}_1\mathscr{A}_2, \tag{42}$$

and $\operatorname{tr} J$ is negative if and only if

$$\mathscr{E}_1+\mathscr{M}_1 < 0, \tag{43}$$

and

$$\mathscr{E}_2+\mathscr{M}_2 < 0. \tag{44}$$

The conditions (43) and (44) are referred to as isoclinic stability of the prey and the predator species, respectively. These conditions equal to convergence stability in single-species evolution. Whenever isoclinic stability holds for both species, it means that the singularity is locally attainable in either direction when the evolution of the other species is absent. In other words, when isoclinic stability holds for the prey species, the singularity is locally attainable if we set $\alpha = \alpha^*$ and assume that the predator evolution is absent. This applies similarly for predator species, when we set $b\tau = b\tau^*$ and assume the absence of prey evolution.

A coevolutionary singularity is *weakly convergence stable* when it is locally attainable for some coefficients $C$ and $D$, so that the inequality (42) holds and also

$$C\cdot(\mathscr{E}_1+\mathscr{M}_1) + D\cdot(\mathscr{E}_2+\mathscr{M}_2) < 0. \tag{45}$$

This essentially implies that at least one of the inequalities (43) or (44) must hold. Then, the singularity is attainable whenever the coefficients $C$ and $D$ satisfy a certain relationship. For example, if $\mathscr{E}_2+\mathscr{M}_2 > 0$ and $\mathscr{E}_1+\mathscr{M}_1 < 0$, then the singularity is attainable if $C/D > -(\mathscr{E}_2+\mathscr{M}_2)/(\mathscr{E}_1+\mathscr{M}_1)$. Observe that whenever $(\mathscr{E}_1+\mathscr{M}_1)(\mathscr{E}_2+\mathscr{M}_2) < 0$, the singularity can only be weakly convergence stable, which also requires that $\mathscr{A}_1\mathscr{A}_2 < 0$.

### 3.4. Critical function analysis

We now investigate the role of the trade-off function $\beta(\alpha)$ in invadability and convergence stability of a coevolutionary singularity. For this investigation, we utilise the critical function analysis of adaptive dynamics (de Mazancourt and Dieckmann 2004; Bowers et al. 2005; Kisdi 2006). The Eq. (29) states that by definition, any singularity $(b\tau^*, \alpha^*)$ satisfies

$$\beta'(\alpha^*) = -\frac{s_1(\alpha^*, \beta(\alpha^*), b\tau^*, \alpha^*, \beta(\alpha^*))}{s_2(\alpha^*, \beta(\alpha^*), b\tau^*, \alpha^*, \beta(\alpha^*))}. \tag{46}$$

We call this the critical slope of the trade-off function $\beta(\alpha)$. In other words, for the trait pair $(b\tau^*, \alpha^*)$ to be a coevolutionary singularity, where the trade-off has the value $\beta(\alpha^*)$ and prey fitness derivative vanishes at $b\tau = b\tau^*$, the trade-off must have the critical slope (46) at $\alpha = \alpha^*$. As similar statement holds also for any boundary attractor $(0, \alpha_0^*)$. Consequently, we may reverse engineer evolutionary singularities by choosing the required slope for the trade-off function.

This recipe for finding coevolutionary singularities requires that $b\tau^*$ exists, but this property is generally uncertain (Lehtinen and Geritz 2019). Indeed, Lehtinen and Geritz demonstrated that for some $\alpha$ and $\beta(\alpha)$, such a value $b\tau^*$ can be absent. This is often the case when catastrophic bifurcations can be encountered through evolution. Thus, critical function analysis for a given ecological environment is applicable only for those combinations of $\alpha$ and $\beta(\alpha)$ for which $b\tau^*$ exists. Assuming such a $b\tau^*$ exists, we can then calculate the values $s_1$ and $s_2$ to obtain the critical slope (46). Moreover, if multiple singular $b\tau^*$ values exist for the same branch of

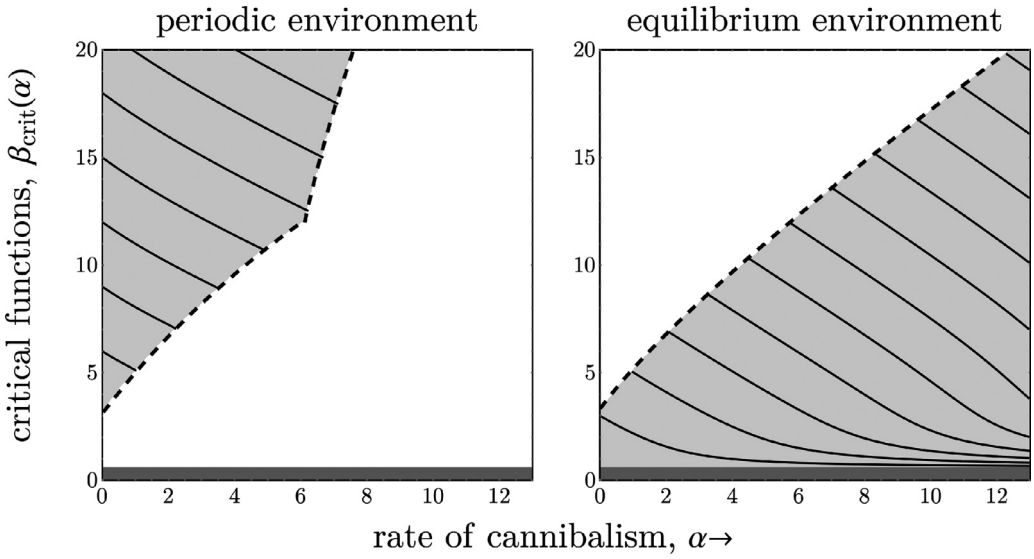


**Fig. 2.** Critical functions as obtained numerically by solving (47) for various initial conditions. Dashed lines indicate where critical functions cease to exist. Dark gray areas depict where the predator is extinct. Parameters are the same as in Fig. 1.

ecological attractors, then there are several critical slopes for the same $\alpha$ and $\beta(\alpha)$, as each $b\tau^*$ produces different $s_1$ and $s_2$. The numerical analysis, however, provides no evidence for this.

The above treatise accounts for a general class of trade-off functions, since only local assumptions are being made about their shape. It follows that both invadability and attainability of a singularity are easily mouldable properties, since they depend on the local curvature of the trade-off function. The value of this curvature affects only the term $\mathscr{E}_2$, which is absent in the singularity conditions. Therefore we can freely tune the curvature to find different outcomes for the same singularity. For instance, since $s_2 \neq 0$, we can always set $\beta''(\alpha^*)$ so that $\mathscr{E}_2$ is negative and the singularity is uninvadable. Finding the trade-off curvature satisfying $\mathscr{E}_2 = 0$, at which the singularity becomes invasible, is also a trivial task. As for the singularity's local attainability, tuning the trade-off curvature affects both of the inequalities (42) and (45). By varying the trade-off curvature, different patterns arise based on whichever of these inequalities is first violated.

Suppose that there exists a function $\psi(\alpha, \beta(\alpha))$ that tracks a given branch of singular $b\tau^*$ values when varying $\alpha$ for a given trade-off $\beta(\alpha)$. A precise definition of $\psi$ has proven elusive. This is due to periodic ecological attractors, which makes finding singular trait values possible only through numerical analysis. A function $\beta_{crit}(\alpha)$ that satisfies the slope of (46) for every $\alpha$ in some interval is called a *critical function*, and is a solution to the differential equation

$$\beta'_{crit}(\alpha) = -\frac{s_1(\alpha, \beta_{crit}(\alpha), \psi(\alpha, \beta_{crit}(\alpha)), \alpha, \beta_{crit}(\alpha))}{s_2(\alpha, \beta_{crit}(\alpha), \psi(\alpha, \beta_{crit}(\alpha)), \alpha, \beta_{crit}(\alpha))}. \tag{47}$$

The solutions of the above equation for different initial conditions form a family of critical functions. The solutions of (47) are defined only as long as the branch of similar ecological attractors exists and the function $\psi$ is well defined. For an arbitrary trade-off function $\beta$, a point $(b\tau, \alpha)$ is singular if the trade-off is tangent to some critical function with $\psi(\alpha, \beta(\alpha)) = b\tau$.

Critical functions were solved numerically using an Euler method with a fixed step-size $\Delta\alpha = 0.05$ for various initial conditions. The process was done separately for equilibrium and periodic environments. At each point of the iteration, we had to solve three values: $b\tau^*$, $s_1$, and $s_2$. We first solved $b\tau^*$ for which the absolute value of the prey fitness derivative is smaller than $10^{-4}$. In the absence of such a value, we checked whether $b\tau^* = 0$ is a viable evolutionary attractor for prey-only evolution. Then, we numerically integrated $s_1$ and $s_2$ for the corresponding ecological environment, and used the critical slope (46) to find the next value $(\alpha, \beta)$ for the iteration. At each step of the iteration, we also collected several other fitness derivatives that are useful later in the analysis, when we search for singularities with desired propertied ($\mathscr{A}_1$, $\mathscr{A}_2$, $\mathscr{E}_1$, $\mathscr{M}_1$, $\mathscr{M}_2$, $s_{11}$, $s_{12}$, $s_{22}$). Observe that of these terms, $\mathscr{A}_1$, $\mathscr{A}_2$, $\mathscr{M}_1$, and $\mathscr{M}_2$ contain derivatives with respect to the resident trait values, causing complications whenever the environment is periodic. These terms were approximated using difference quotients for the intervals $[b\tau^* - \Delta b\tau, b\tau^* + \Delta b\tau]$ and $[\alpha^* - \Delta\alpha, \alpha^* + \Delta\alpha]$ with $\Delta b\tau = \Delta\alpha = 10^{-4}$, and where the trade-off function was approximated using the linear function $\beta(\alpha) = \beta(\alpha^*) + \alpha\beta'(\alpha^*)$.

## 4. Predator-prey coevolution

### 4.1. Emergence of cannibalism

We begin the coevolutionary analysis by investigating the conditions under which cannibalism emerges. Namely, we investigate how such emergence is influenced by the trade-off relationship between prey and juvenile capture, and the evolution of timidity of the prey. As before, we assume that favouring cannibalism has a decreasing effect on success in prey capture. In other words, the rate of prey capture is maximised in the absence of cannibalism. Throughout this section, we assume that cannibalism is absent, $\alpha = 0$. Recall that in the absence of cannibalism, there is no ecological bistability, and the level of timidity and the rate of prey capture uniquely determine the ecological environment.

A simple classification for the emergence of cannibalism can be constructed from three ingredients. The first depends on the value and slope of the trade-off function $\beta(\alpha)$ at $\alpha = 0$. The second depends on whether a mutant predator type with small $\alpha_m > 0$ can invade for a given level of timidity of the prey, $b\tau$. The third depends on the level of timidity $b\tau^*$ that the prey attains through evolution while cannibalism is absent. Using these three ingredients, we classify four qualitative different ways in which cannibalism emerges as a response to timidity of the prey.

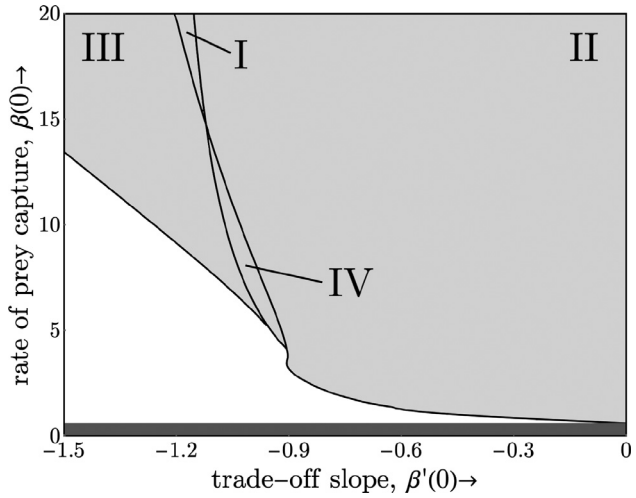


**Fig. 3.** Numerical illustration of type I-IV evolutionary responses of cannibalism to timidity of the prey. In the white region cannibalism is always unfavourable. Parameters are the same as in Fig. 1.

(I) $[\partial s/\partial \alpha_m]_{\alpha_m=0} > 0$ for $b\tau = 0$, and $[\partial s/\partial \alpha_m]_{\alpha_m=0} < 0$ for $b\tau = b\tau^*$.

(II) $[\partial s/\partial \alpha_m]_{\alpha_m=0} > 0$ for $b\tau = 0$ and $b\tau = b\tau^*$.

(III) $[\partial s/\partial \alpha_m]_{\alpha_m=0} < 0$ for $b\tau = 0$ and $b\tau = b\tau^*$, and there exists $\Omega \subset (0, b\tau^*)$ such that $[\partial s/\partial \alpha_m]_{\alpha_m=0} > 0$ for all $b\tau \in \Omega$.

(IV) $[\partial s/\partial \alpha_m]_{\alpha_m=0} < 0$ for $b\tau = 0$, and $[\partial s/\partial \alpha_m]_{\alpha_m=0} > 0$ for $b\tau = b\tau^*$.

The above classifications help distinguish how simultaneous prey evolution affects the emergence of cannibalism. For evolutionary response of type I, the outcome is possible in the absence of timidity, but prey evolution eventually makes cannibalism unfavourable. Hence, this scenario predicts when prey evolution reduces the chances of cannibalism to emerge. For response of type II, cannibalism is always going to emerge, and the end result is unaffected by the prey evolution. On the other hand, for responses of type III and IV, prey evolution is necessary for cannibalism to be favourable, which occurs after the prey has attained sufficiently high level of timidity.

Observe that for the response of type III, there is an evolutionary 'window' during which cannibalism is favourable, but eventually prey evolution makes it unfavourable. Whether cannibalism is expected to evolve during that window depends on the relative speeds of prey and predator evolution. However, even if predators do attain positive levels of cannibalism during that window, the rate of cannibalism is expected to attain relatively low value due to small evolutionary steps. Consequently, the general course of prey evolution remains largely unaffected, and which eventually causes cannibalism to vanish through predator evolution. Therefore, this scenario predicts when cannibalism is only a transient stage of evolution.

To investigate how the emergence of cannibalism depends on the trade-off properties, we set $\alpha = 0$ and apply the following numerical procedure. For each value of $\beta(0)$, we first solve the singular value $b\tau^*$. Then, for each fixed trade-off slope $\beta'(0)$, we vary $b\tau \in [0, b\tau^*]$ and collect the values of the fitness derivative $[\partial s/\partial \alpha_m]_{\alpha_m=0}$. For the data behind Fig. 3, we used the step sizes $\Delta b\tau = b\tau^*/10$, $\Delta\beta(0) = 0.01$, and $\Delta\beta'(0) = 0.0075$.

Numerical analysis reveals that all four types of evolutionary responses are possible. Fig. 3 presents a typical example of how the emergence of cannibalism is influenced by the trade-off slope and the rate of prey capture. When the trade-off slope is steep so that $\beta'(0)$ is large negative, cannibalism can never emerge. When the trade-off is less steep, emergence of cannibalism eventually becomes possible. Sufficiently flat trade-offs ($\beta'(0) \approx 0$) often result in type II response, as there is only little cost for cannibalism.

In general, lowering the rate of prey capture or increasing the steepness of the trade-off hinder the emergence of cannibalism. For low rates of prey capture ($\beta(0) < 4.1$), positive levels of timidity are always unfavourable, hence $b\tau^* = 0$ and only type II response can occur. The supercritical Hopf bifurcation of the ecological dynamics occurs at $\beta(0) = 3.5$, above which the ecological environment is at a periodic attractor. In Fig. 3, this bifurcation causes the 'hump' in the boundary of type II response.

For higher rates of prey capture ($\beta(0) > 4.1$) evolutionary responses of types I, III, and IV are also possible. Response of type I and IV, however, occurred only rarely. Furthermore, type IV response is unattainable for $\beta(0) > 14.65$, while type I is unattainable for $\beta(0) < 14.65$. When crossing the intersection between all different types I-IV ($\beta(0) = 14.65$, $\beta'(0) = -1.12$), the qualitative differences of predator evolution occurs at the boundaries $b\tau = 0$ and $b\tau = b\tau^*$, as described by the definitions above, and for the intermediate values cannibalistic predator mutants can invade.

To explain why cannibalism is more likely to emerge for high rates of prey capture, recall that in the present study the only cost of cannibalism is the decreased rate of prey capture. Although the rate of prey capture is decreased by the same absolute value, the relative decrease differs between initially high and low rates. In other words, predators who are already unsuccessful in capturing the prey have more to lose if they turn to cannibalism.

### 4.2. Evolutionary branching

We now investigate evolutionary branching of the cannibalistic predator species. When only predator evolution is present, a locally attainable and invasible singularity is an evolutionary branching point (Geritz et al. 1998). But when the prey and the predator species coevolve, the coexistence of two similar trait types is a separate requirement for evolutionary branching (Kisdi 2006). Coevolution further yields three different types of branching points, since the coevolutionary singularity may give rise to branching of either the prey or the predator species, or both of them. The numerical analysis, however, provides no evidence for evolutionary branching of the prey species. Thus, we focus on the conditions under which the predator branches into two types with different rates of cannibalism.

Suppose that $(b\tau^*, \alpha^*)$ is a coevolutionary singularity. For simplicity, throughout this section we assume that isoclinic stability holds for the prey species, so that $\mathscr{E}_1 + \mathscr{M}_1 < 0$. In the numerical analysis this inequality was always found to hold. For the singularity to be a branching point for the predator species, three conditions must be met. Firstly, the singularity must be locally attainable through evolution. Secondly, mutant predator types with either lower or higher rates of cannibalism must be able to invade, so that the selection becomes disruptive. Thirdly, in the vicinity of the singularity two predator types must be able to coexist and mutually invade each other. Otherwise the mutant type simply replaces the resident, and branching is absent even under disruptive selection. Thus, the singularity $(b\tau^*, \alpha^*)$ is an evolutionary branching point for the predator species if and only if the following inequalities hold:

$$\mathscr{E}_2 + \mathscr{M}_2 < \mathscr{A}_1\mathscr{A}_2/(\mathscr{E}_1 + \mathscr{M}_1), \tag{48}$$

$$\mathscr{E}_2 + \mathscr{M}_2 < -(\mathscr{E}_1 + \mathscr{M}_1)\cdot C/D, \tag{49}$$

$$\mathscr{E}_2 > 0, \tag{50}$$

$$\mathscr{M}_2 < 0. \tag{51}$$

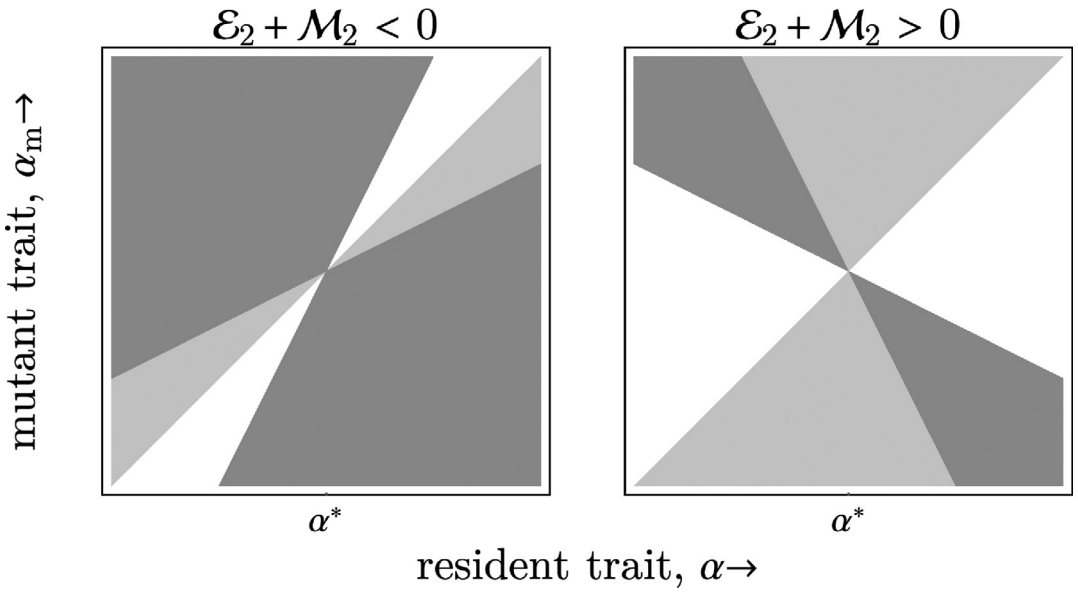


**Fig. 4.** Graphical illustration of pairwise invasibility plots for the predator in the vicinity of qualitatively different branching points. Gray regions depict where invasion is possible, and dark gray depicts where mutual coexistence is possible. In both panels, the coevolutionary singularity is at $(b\tau^*, \alpha^*) = (1.322, 1.5)$, with $\beta(\alpha^*) = 13.4858$ and $\beta'(\alpha^*) = -0.9194$. Isoclinic stability holds for the prey species, $\mathcal{E}_1 + \mathcal{M}_1 = -0.247$, and $\mathcal{M}_2 = -0.003$, $\mathcal{A}_1\mathcal{A}_2 = -0.0001$. *Left:* $\beta''(\alpha^*) = 0.04$, $\mathcal{E}_2 + \mathcal{M}_2 = -0.0013$, hence isoclinic stability holds for the predator species. *Right:* $\beta''(\alpha^*) = 0.08$, $\mathcal{E}_2 + \mathcal{M}_2 = 0.0002$, hence isoclinic stability is lacking for the predator species. The narrow cone of coexistence in the right panel leads to delayed evolutionary branching. Parameters are the same as in Fig. 1.

The sign of the product $\mathcal{A}_1\mathcal{A}_2$ affects the conditions that are necessary for evolutionary branching. When $\mathcal{A}_1\mathcal{A}_2 > 0$, the inequality (48) requires that isoclinic stability necessarily holds for the predator species as well, that is, $\mathcal{E}_2 + \mathcal{M}_2 < 0$. In other words, any singularity satisfying $\mathcal{A}_1\mathcal{A}_2 > 0$ can be a branching point only if it is strongly convergence stable.

When $\mathcal{A}_1\mathcal{A}_2 < 0$, isoclinic stability may be lacking for the predator species while still resulting in evolutionary branching. This is because the sum $\mathcal{E}_2 + \mathcal{M}_2$ may be either positive or negative and still satisfy (48). When $\mathcal{E}_2 + \mathcal{M}_2 < 0$ and $\mathcal{E}_2 > 0$, the singularity is an evolutionary branching point independent of simultaneous prey evolution: neither slow nor rapid prey evolution can prevent branching of the predator. Rapid prey evolution does, however, quicken convergence to the singularity. But when $\mathcal{E}_2 + \mathcal{M}_2 > 0$, simultaneous prey evolution is necessary for the convergence. This occurs when either the coefficient $C$ is large or $D$ is small. In other words, slow predator evolution can be compensated by rapid prey evolution to retain the singularity's attainability. As a conclusion, for $\mathcal{A}_1\mathcal{A}_2 < 0$ weak convergence stability is sufficient for evolutionary branching of the predator, and depending on the sign of $\mathcal{E}_2 + \mathcal{M}_2$, this may require relatively rapid prey evolution.

Whenever rapid prey evolution is necessary for the singularity's attainability, evolutionary branching is predicted to be delayed. This delay concerns the process of converging to the branching point and the coevolutionary dynamics between one prey and two coexisting predator types after branching. The reasons for the delay are as follows. Firstly, when isoclinic stability holds for the prey but is lacking for the predator species, every successful mutant predator type pulls evolutionary trajectories away from the singularity. On the other hand, successful prey mutants do the opposite and tend towards the singularity. For sufficiently rapid prey evolution, the singularity is attained in the long-run, but these opposing 'forces' delay the process.

The second reason for the delay is that after branching has occurred, there is only a narrow cone of mutual coexistence (less than right angle). This, again, is a consequence of the lack of isoclinic stability. Therefore, any further successful predator mutations are likely to appear outside the cone, whereupon the other resident type goes extinct. In addition, the branching process may also cause the environment to exert different selection pressure on the prey. If so, the prey evolves away from $b\tau^*$, which alters the cone of coexistence so that one of the predator types goes extinct. In other words, evolutionary branching is often followed by chance extinction of one of the resident types. After each unsuccessful branching, in which coexistence lasted only for a brief moment in the evolutionary timescale, the evolutionary dynamics revert back to the original scenario with one prey and predator type present. Eventually this process is expected to succeed so that coexistence is unlikely to perish so easily, and the two predator types are clearly distinct in their cannibalistic behaviour.

The two panels in Fig. 4 illustrate the difference between typical (*left*) and delayed (*right*) evolutionary branching. In both of these examples, the level of timidity of the prey is fixed at $b\tau = b\tau^*$ and only the predator is evolving. The only difference is the assumed trade-off curvature at the singularity. Gray regions depict which mutant predator type $\alpha_m$ can invade a given resident $\alpha$, that is, $s(\alpha_m, \beta(\alpha_m), b\tau^*, \alpha, \beta(\alpha)) > 0$. Furthermore, dark gray regions depict where invasion is also possible if the roles are switched, so that $s(\alpha, \beta(\alpha), b\tau^*, \alpha_m, \beta(\alpha_m)) > 0$. Mutual coexistence between two nearby predator traits is possible only in the dark gray regions.

In the left panel of Fig. 4 the cones of mutual coexistence are broad (greater than right angle), and conversely narrow in the right panel. In particular, if one could fix the resident predator trait exactly at the singular value $\alpha = \alpha^*$, then in both cases any mutant type can invade. For a broad cone, a successful invasion by a mutant implies coexistence with the resident. However, for a narrow cone such coexistence is unattainable when the resident is at $\alpha^*$. This is because any successful mutant would simply replace the resident type. Mutual coexistence can hence be achieved only if the resident type is slightly away from the singularity, and if the successful mutant type belongs to the narrow cone.

Let us now focus on the role of trade-off curvature. Observe that in the conditions (48)–(51), only the term $\mathcal{E}_2$ depends on the trade-off curvature $\beta''(\alpha^*)$, as described by (35). Moreover, the conditions for $(b\tau^*, \alpha^*)$ to be a coevolutionary singularity, (28) and

(29), are also independent of this curvature. This essentially means that the trade-off curvature can be treated as a free variable, and by varying it we obtain different evolutionary outcomes for the same singularity, such as evolutionary branching.

Whenever the trade-off curvature is sufficiently concave, the conditions (48) and (49) are met, and $\mathscr{E}_2 < 0$. In other words, when $\beta''(\alpha^*)$ is large negative, the singularity is convergence stable and no mutants can invade. By increasing $\beta''(\alpha^*)$ the singularity loses convergence stability when either (48) or (49) is violated, and becomes invasible when $\mathscr{E}_2 = 0$. Whenever $\mathscr{M}_2 > \mathscr{A}_1\mathscr{A}_2/(\mathscr{E}_1 + \mathscr{M}_1)$ holds at singularity, the loss of convergence stability occurs before it becomes invasible. If the singularity retains convergence stability at $\mathscr{E}_2 = 0$, and also $\mathscr{M}_2 < 0$ holds, then there is an interval of trade-off curvatures that yield an evolutionary branching point.

Based on the observations above, we can construct a simple recipe for finding evolutionary branching points. First, one should seek for evolutionary singularities for which $\mathscr{M}_2 < \min\{0, \mathscr{A}_1\mathscr{A}_2/(\mathscr{E}_1 + \mathscr{M}_1)\}$. Then, any such singularity can be turned into a branching point by tuning the trade-off curvature $\beta''(\alpha^*)$ so that $\mathscr{E}_2$ becomes small positive. Further increasing the curvature causes the singularity to lose convergence stability, whereupon it is no longer a branching point. Evolutionary branching occurs for the intermediate trade-off curvatures between the possibility of invasion and the loss of convergence stability.

In a similar fashion, we can construct a recipe for delayed evolutionary branching. Recall that at the loss of isoclinic stability, the singularity remains convergence stable only when $\mathscr{A}_1\mathscr{A}_2 < 0$. By further increasing trade-off curvature, the convergence stability is retained as long as both (48) and (49) hold. In other words, as long as (48) holds, the singularity is a delayed evolutionary branching point whenever the relation $C/D$ is sufficiently large.

The above recipe, together with critical function analysis, provided a straightforward method for finding evolutionary branching points. After solving critical functions numerically, we simply looked for singularities with the desired properties. Recall that critical functions are solutions of the differential Eq. (47). For a simple demonstration, consider the critical function corresponding to the initial condition $(\alpha_0, \beta_{crit}(\alpha_0)) = (0, 15)$. The curve of such a critical function is visible in the left panel of Fig. 2, and ceases to exist at $\alpha^* = 4.85$. The level of timidity of the prey along the critical curve ranges from $b\tau^* = 2.3865$ to $b\tau^* = 0$, respectively, for $\alpha^* = 0$ and $\alpha^* = 4.85$. The term $\mathscr{M}_2$ is negative for $\alpha^* < 1.81$, and positive for $\alpha^* > 1.81$. Similarly, the term $\mathscr{A}_2$ is negative for $\alpha^* < 1.43$, and positive for $\alpha^* > 1.43$, while $\mathscr{A}_1$ is always negative. Therefore, one readily sees that for the singularities along this critical curve, evolutionary branching is possible for $\alpha^* < 1.81$. For $1.43 < \alpha^* < 1.81$, also delayed evolutionary branching is possible.

To illustrate how varying the trade-off curvature affects invasibility and convergence stability, we consider three singularities along the critical function of the example above. These observations motivate us to choose $\alpha^* = 1$, $\alpha^* = 1.5$, and $\alpha^* = 3$, since they yield qualitatively different outcomes when the trade-off curvature varies. Evolutionary branching is possible in the first two singularities, whereas in the third singularity it is impossible. Moreover, only the second singularity allows for delayed branching. Fig. 5 depicts evolutionary bifurcation diagrams when the trade-off curvature $\beta''$ and the relationship $C/D$ vary. For $\alpha^* = 1$, the level of timidity is $b\tau^* = 1.631$, and the trade-off has the value $\beta(1) = 13.9582$ and the slope $\beta'(1) = -0.9714$. The second order fitness derivatives have the values $\mathscr{A}_1 = -0.1229$, $\mathscr{A}_2 = -0.0066$, $\mathscr{E}_1 = -0.0085$, $\mathscr{M}_1 = -0.1868$, and $\mathscr{M}_2 = -0.0088$. The singularity is strongly convergence stable for $\beta''(1) < 0.2288$, otherwise it is repelling. The singularity is uninvadable for $\beta''(1) < -0.0021$, otherwise it can be invaded by mutant types. Therefore, evolutionary branching occurs for $-0.0021 < \beta''(1) < 0.2288$. In this example, delayed branching is absent.

For $\alpha^* = 1.5$, the level of timidity is $b\tau^* = 1.3223$, and the trade-off has the value $\beta(1.5) = 13.4858$ and the slope $\beta'(1.5) = -0.9194$. The second order fitness derivatives have the values $\mathscr{A}_1 = -0.1383$, $\mathscr{A}_2 = 0.0009$, $\mathscr{E}_1 = -0.0100$, $\mathscr{M}_1 = -0.2370$, and $\mathscr{M}_2 = -0.0030$. The singularity is uninvadable for $\beta''(1.5) < -0.0036$, and weakly convergence stable for $\beta''(1.5) < 0.0886$. Strong convergence stability occurs for $\beta''(1.5) < 0.0750$. Therefore, evolutionary branching without delay occurs for $-0.0036 < \beta''(1.5) < 0.0750$. For $0.0750 < \beta''(1.5) < 0.0886$, the singularity is locally attainable only if $C/D$ is sufficiently large, whereupon evolutionary branching is delayed.

Finally, for $\alpha^* = 3$, the level of timidity is $b\tau^* = 0.5984$, and the trade-off has the value $\beta(3) = 12.1909$ and the slope $\beta'(3) = -0.8173$. The second order fitness derivatives have the values $\mathscr{A}_1 = -0.2236$, $\mathscr{A}_2 = 0.0315$, $\mathscr{E}_1 = -0.0162$, $\mathscr{M}_1 = -0.5597$, and $\mathscr{M}_2 = 0.0107$. The singularity is uninvadable for $\beta''(3) < -0.0072$, and weakly convergence stable for $\beta''(3) < 0.0322$. Strong convergence stability occurs for $\beta''(3) < -0.287$. Therefore, the singularity can be invaded by mutants for $-0.0072 < \beta''(3) < 0.0322$. But since $\mathscr{M}_2$ is positive, evolutionary branching is absent as nearby mutants are unable to coexist with the resident.

### 4.3. Evolutionary cycles

We now investigate evolutionary cycles driven by two qualitatively different mechanisms. First, we analyse genetically driven cycles that arise through a supercritical Hopf bifurcation of the canonical Eq. (27). Then, we analyse ecogenetical cycles driven by abrupt shifting between alternative ecological attractors.

Assume that $\mathscr{E}_1 + \mathscr{M}_1 < 0$, as before. Then, a coevolutionary singularity $(b\tau^*, \alpha^*)$ undergoes a supercritical Hopf bifurcation when

$$\mathscr{E}_2 + \mathscr{M}_2 < \mathscr{A}_1\mathscr{A}_2/(\mathscr{E}_1 + \mathscr{M}_1), \tag{52}$$

$$\mathscr{E}_2 + \mathscr{M}_2 = -(\mathscr{E}_1 + \mathscr{M}_1) \cdot C/D. \tag{53}$$

It follows that a Hopf bifurcation is possible only for weakly convergence stable singularities, because the equations above require that $\mathscr{E}_2 + \mathscr{M}_2 > 0$ and $\mathscr{A}_1\mathscr{A}_2 < 0$. Assume that the latter inequality holds. Then, by tuning the local trade-off curvature $\beta''$, we can always find a value of $\mathscr{E}_2$ satisfying (52). After fixing any such value, there exists a unique $C/D$ satisfying (53). Therefore, whenever $\mathscr{A}_1\mathscr{A}_2 < 0$ holds at a singularity, genetical cycles through Hopf bifurcation can always be achieved by tuning $\beta''$ and $C/D$.

The centre and right panels of Fig. 5 illustrate Hopf bifurcation of the canonical equation for two different singularities. In the centre panel, a delayed evolutionary branching point can undergo Hopf bifurcation for $\beta'' \in (0.0750, 0.0886)$. When $\beta'' > 0.0886$, the inequality (52) is violated and Hopf bifurcation of the canonical equation is impossible. In the right panel, evolutionary branching is absent and the singularity can undergo Hopf bifurcation for $\beta'' \in (-0.2870, 0.0322)$. When $\beta'' > 0.0322$, Hopf bifurcation is impossible.

Next, we consider ecogenetical cycles driven by ecological attractor switching. The idea, briefly, is that when evolution causes an ecological attractor to disappear through a catastrophic bifurcation, the environment switches to an alternative attractor. Although the evolving traits have changed only slightly in the process, the selection for the prey and the predator species can be substantially different in this alternative environment. Consequently, the directions of prey and predator evolution can take an abrupt and unpredicted shift. Under this alternative environment, the process of encountering a catastrophic bifurcation may eventually occur yet again, shifting the environment back to the original environment. When this whole process occurs recurrently following a distinguishable pattern, the long-term evolution is cycling.

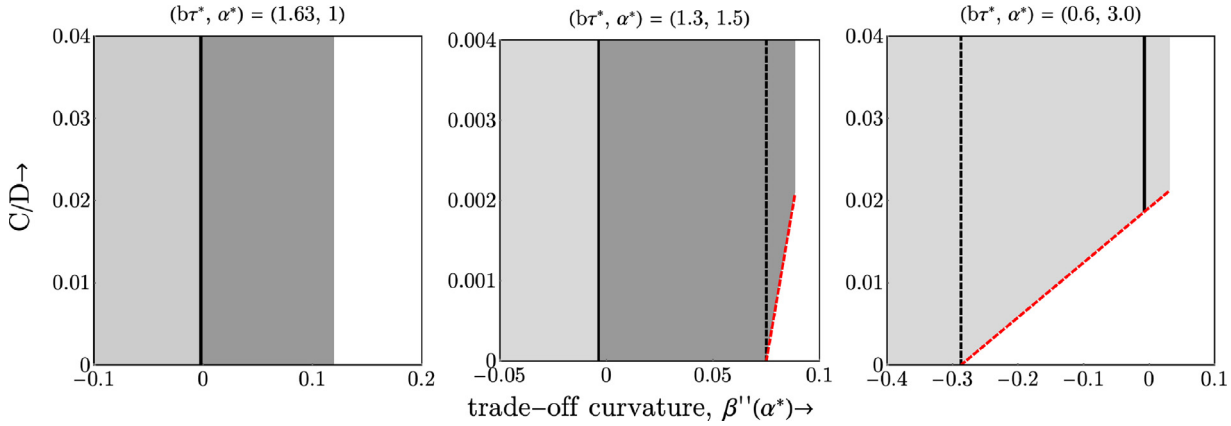


**Fig. 5.** The effect of trade-off curvature and relative speed of evolution on evolutionary outcomes. In all panels, gray areas indicate when the singularity is convergence stable, otherwise it is repelling. Dark gray areas correspond to evolutionary branching. Black thick line: $\mathscr{E}_2 = 0$; Black dashed line: $\mathscr{E}_2 + \mathscr{M}_2 = 0$; Red dashed line: Hopf bifurcation of the canonical equation. *Left:* $\mathscr{A}_1\mathscr{A}_2 > 0$, $\mathscr{M}_2 < 0$. *Centre:* $\mathscr{A}_1\mathscr{A}_2 < 0$, $\mathscr{M}_2 < 0$. *Right:* $\mathscr{A}_1\mathscr{A}_2 < 0$, $\mathscr{M}_2 > 0$. For definitions of these terms, see (36)–(41). Parameters are the same as in Fig. 1.

Such an ecogenetically driven cycle thus comprises two ingredients: intermediate phases in different ecological environments, and ecological attractor switchings connecting these phases.

Recall that our ecological model exhibits bistability between periodic and equilibrium attractors. When bistability is present, the equilibrium environment vanishes through a subcritical Hopf bifurcation on the ecological timescale, and the periodic environment similarly vanishes through a fold bifurcation of limit cycles. When predator evolution is absent, the evolution of prey is sufficient to cause recurrent ecological attractor switching leading to cyclic evolution (Lehtinen and Geritz 2019). Lehtinen and Geritz demonstrated that to find such attractor switching cycles, one only needs to look for branches of ecological attractors in which evolution never comes to a stasis. Since runaway selection was absent in that model, this implied continual switching between the two ecological attractors through evolution.

In the case of predator-prey coevolution, ensuring the existence of ecogenetically driven cycles is more complicated. This is because the existence of ecological bistability is near impossible to guarantee without resorting to numerical analysis, even in the absence of trade-off (Lehtinen and Geritz 2019). At the same time, the trade-off function $\beta(\alpha)$ affects the global dynamics of evolution in a largely unpredictable manner. The task of choosing a trade-off that satisfies the desired ecological and evolutionary properties is hence ever more challenging. In addition, we have no information about the coefficients $C$ and $D$ in the canonical Eq. (27). While critical function analysis is useful when dealing with local properties of evolutionary singularities, it provides little assistance here as we need to know the global shape of the trade-off.

To find ecogenetical cycles, we rely on graphical phase-plane analysis. This is based on investigating the geometries of evolutionary isoclines, in which either the prey or the predator fitness derivative vanishes. The direction of evolution is guided by the fitness derivatives, and thus the general evolutionary trends are the same in the regions bounded by the isoclines. Studying the geometries of these isoclines is a fruitful endeavour, as they reveal whether evolutionary cycles are possible in the first place.

By applying the phase-plane analysis for different trade-off functions, we found many examples of evolutionary cycles driven by ecological attractor switching. The trade-off functions were constructed using the *Interpolation* function of *Mathematica*®. Trade-off functions that resembled a smoothed step function often produced complex isocline geometries and several evolutionary singularities. As a demonstration, one might construct a trade-off function with the following points and slopes: $(\alpha, \beta) = (0, 22)$ with

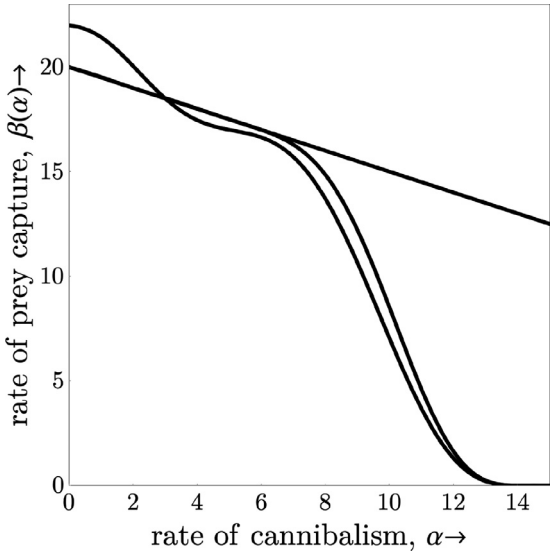


**Fig. 6.** Three possible trade-off functions.

the slope $\beta' = -0.25$; (3, 18.5); (5, 17); (7, 15.7); (14, 0) with the slope $\beta' = 0$; and (15, 0) with the slope $\beta' = 0$. This trade-off produces three evolutionary singularities and ecological attractor switching cycles are also possible (data not shown). In the present work, however, we focus on trade-offs for which the isocline geometries are considerably simpler. These include a linear trade-off, and a trade-off that is initially linear but has a steep tail. Fig. 6 shows a comparison between the shapes of these three trade-off functions.

As a first example, we choose a linear trade-off function: $\beta(\alpha) = 20 - 0.5\alpha$, when $\alpha \in [0, 40]$, otherwise it is zero. Fig. 7(a) provides a phase-plane demonstration of the evolutionary dynamics. The black arrows indicate the general direction of evolution within the regions bounded by the isoclines. For this trade-off, there is one evolutionary uninvadable singularity at $(b\tau^*, \alpha^*) = (0, 35.5)$ corresponding to the equilibrium environment and with $\beta(35.5) = 2.25$ (not shown in the figure). No other singularities or boundary attractors exist for this trade-off function. For any initial point in the trait-space with $\alpha > 8.72$, the long-term evolutionary dynamics always attain that singularity. On the other hand, if the threshold value $\alpha = 8.72$ is never encountered, then all trajectories that start below that value remain bounded. This

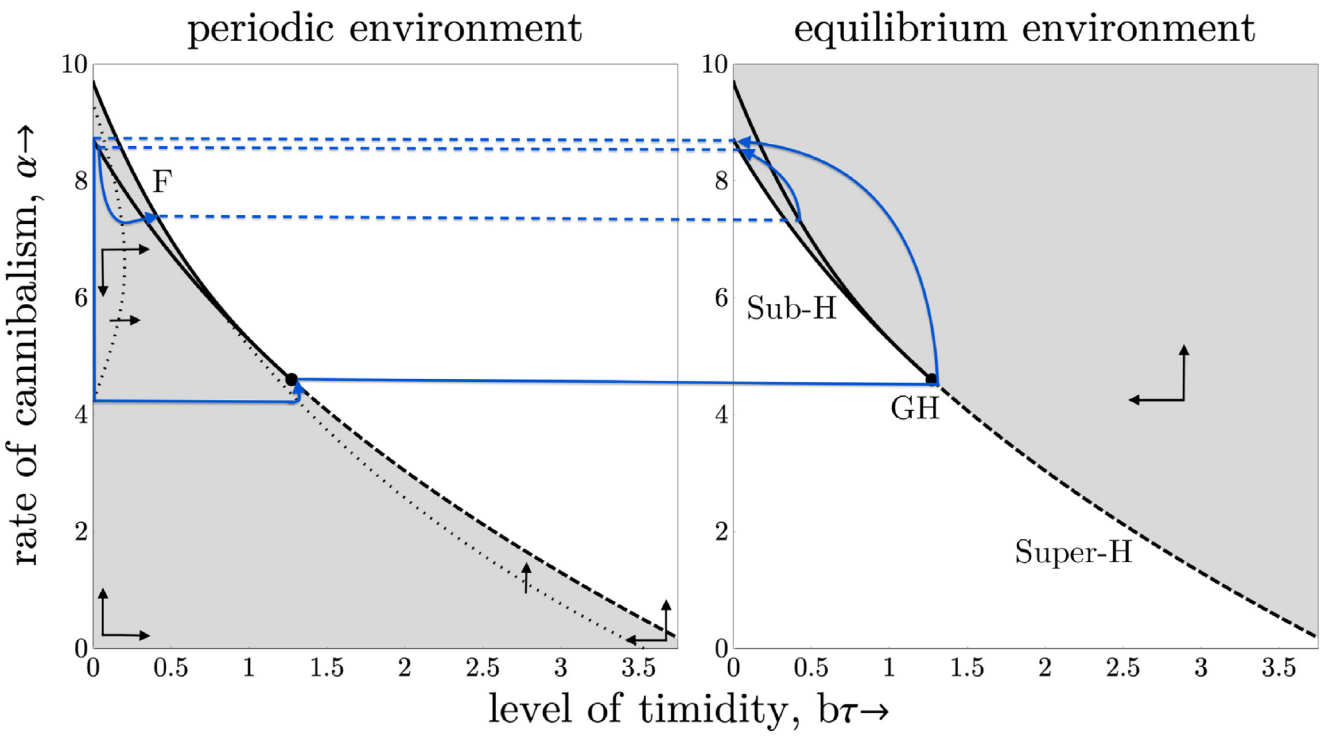


(a) Linear trade-off function $\beta(\alpha)$.

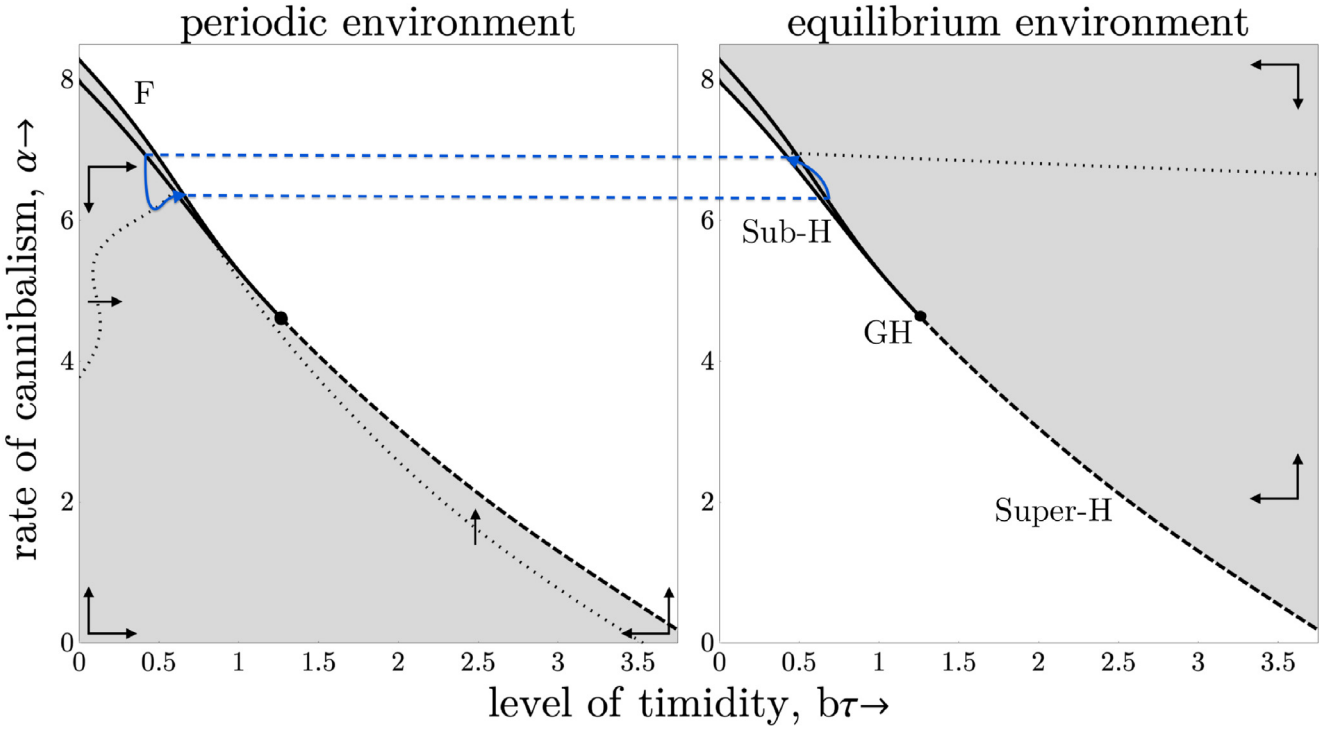


(b) Initially linear trade-off function $\beta(\alpha)$, but with a steep tail.

**Fig. 7.** Coevolutionary dynamics of prey and predator traits for two different trade-off functions. Thin dotted lines indicate isoclines of fitness derivatives. Blue lines are graphical illustrations of evolutionary cycles driven by ecological attractor switching, where the switches are shown in dashes. The boundaries at which supercritical Hopf, subcritical Hopf, and fold bifurcations of ecological dynamics occur are denoted by, respectively, super-H, sub-H, and F. The generalised Hopf is denoted by GH. Parameters are the same as in Fig. 1.

can be achieved by, for example, assuming that $D$ is negligible at $\alpha = 8.72$. It follows that all evolutionary trajectories beginning in this bounded region attain a cyclic attractor. Therefore, even without any knowledge about the complicated coefficients $C$ and $D$ below $\alpha = 8.72$, we can already deduce the qualitative behaviour of long-term coevolution. Admittedly, the assumption made about the coefficient $C$ at $\alpha = 8.72$ is unjustifiable, and suggests that the problem of characterising meaningful conditions resulting in attractor switching cycles is far from easy.

As a second example, we tune the linear trade-off so that long-term coevolution is always cyclic. In particular, we want to refrain from making any assumptions about the coefficients $C$ and $D$, and at the same time, ensure that evolutionary trajectories remain bounded. It turns out that this is easily achieved by modifying the linear trade-off to have a steep tail. For this purpose, we construct a trade-off with the following points and slopes: $(\alpha, \beta) = (0, 20)$ with the slope $\beta' = -0.5$; (2, 19) with the slope $\beta' = -0.5$; (5, 17.5) with the slope $\beta' = -0.5$; (6, 17); (10, 8); (14, 0) with the slope $\beta' = 0$; and (15,0) with the slope $\beta' = 0$.

Fig. 7(b) provides a phase-plane demonstration of the evolutionary dynamics when the initially linear trade-off has a steep tail. Naturally, the dynamics are equivalent to the previous example as long as the trade-off is linear. At around $\alpha = 4$, the modified trade-off begins to deviate gradually from the linear trade-off, resulting in slightly different isocline geometries. For $\alpha > 7$, the modified trade-off is sufficiently steep that the predator's fitness derivative is always negative. Hence, evolutionary trajectories remain bounded. As there are neither singularities nor boundary attractors in the whole trait-space, all evolutionary trajectories converge to an attractor switching cycle for any $C$ and $D$.

The blue lines in Fig. 7(a) and (b) are graphical illustrations of evolutionary cycles driven by ecological attractor switching. Dashed lines depict abrupt attractor switchings between alternative ecological environments. Many other similar illustrations are easy to produce for the same figures, as the recipe for such cycles is rather straightforward. One simply has to find two evolutionary trajectories along each ecological environment, as guided by the black arrows, so that these trajectories connect at the bifurcation points and form a closed path. Furthermore, Fig. 7(a) demonstrates two qualitatively different attractor switching cycles, which are present simultaneously. A full evolutionary cycle can undergo an abrupt attractor switch either once or twice.

An evolutionary cycle containing only one attractor switch does so through subcritical Hopf bifurcation of the ecological dynamics. In the trait-space the cycle orbits the generalised Hopf bifurcation of the ecological dynamics, and the subcritical Hopf bifurcation causes the environment to shift from equilibrium to periodic attractor. Eventually, the environment shifts back to the equilibrium attractor smoothly through supercritical Hopf bifurcation. For the evolutionary cycle in 7(a), the point of supercritical Hopf is very close to the generalised Hopf bifurcation. We found these kinds of cycles to be rare, and they usually required extreme evolutionary trajectories.

For an evolutionary cycle containing two attractor switches, there is no smooth bifurcations nor orbiting around the generalised Hopf bifurcation of the ecological dynamics. The attractor switches are caused in turn by subcritical Hopf and fold bifurcations. These cycles are also possible in single species evolution, where the evolutionary trajectories correspond to either horizontal or vertical lines in the trait-space. For the linear trade-off of Fig. 7(a), however, only prey evolution allows such a cycle. This is because predator evolution is unable to cause subcritical Hopf bifurcation. On the other hand, for the modified trade-off of Fig. 7(b), either prey or predator evolution alone is enough to cause this type of attractor switching cycle.

## 5. Discussion

We have left many complications out of our simple model, such as a continuum of individual sizes or handling time for cannibalism. The analysis is, however, sufficient to show that coevolution can explain how cannibalism emerges as an evolutionary response to timidity of the prey. Also, if cannibalism is steeply traded off with the prey capture, such behaviour can never emerge through predator evolution. Clearly, there is no general rule in nature to say that timid prey behaviour would lead to cannibalistic predators, as the emergence depends on the properties of both the trade-off relationship and the ecological environment. Furthermore, long-term coevolution easily leads to a wide range of evolutionary outcomes, including evolutionary branching and several kinds of evolutionary cycles. Evolutionary cycles are, apparently, a natural outcome of coevolution.

The analysis demonstrates that, for gently sloping trade-offs, cannibalism emerges without simultaneous prey evolution, while it is necessary when the trade-off is steep. For steeper trade-offs, cannibalism is more likely to be only a transient stage of evolution than a lasting outcome (type III and IV in Fig. 3). Curiously, prey evolution towards higher levels of timidity can also make cannibalism unfavourable (type I). In other words, this describes a scenario in which cannibalism is favourable when the prey are always available, while limiting prey availability hinders cannibalism. These findings may help to explain why cannibalism appears in contrasting prevalences between species (Fox 1975). Dercole and Rinaldi (2002) came to similar conclusions using a different modelling approach, in which they found highly cannibalistic predators to encounter evolutionary extinction. Unfortunately, the present work can only offer an explanation insofar as species behave according to our ecological assumptions. More detailed explanations for cannibalism in certain species require models tailor-made for their specific ecosystem.

The trade-off for cannibalism posed in the present work, as decreased success in prey capture, is unlikely to be the only one. If the victims of cannibalism are able to defend themselves, the potential costs also include risk of injury or death in a fight, as in the chimpanzee *Pan troglodytes* (Goodall 1977). In the larvae of several amphibian species, such as the salamander *Hynobius retardatus*, cannibalistic individuals have larger heads that allows them to feed on smaller conspecifics. Due to the increased energetic cost associated with growth, cannibalism tends to be beneficial only in high-density amphibian populations (Kohmatsu et al. 2001; Wakano et al. 2002). The present work assumes that the victims are sufficiently small so that the handling time is negligible. But if there is a handling time, the benefits of cannibalism are likely hindered by the additional time spent handling (Getto et al. 2005). Consequently, cannibalism is less likely to emerge and requires high conversion efficiency.

Evolutionary branching of cannibalistic predators is surprisingly common in our model. In contrast, for the evolution of handling time with a trade-off between conversion efficiency, evolutionary branching appears less likely (Geritz et al. 2007). While Geritz et al. (2007) assumed no cannibalism, it would be interesting to see whether a fixed rate of cannibalism promotes evolutionary branching of handling time. Furthermore, the present work focuses on the conditions under which evolutionary branching occurs, but this only scratches the surface. The long-term coevolution could, for example, lead to stable coexistence between two predator types or further branching into three types.

To explain coexistence of two predator types, consider a prey specialist and a highly voracious cannibal. When only the prey specialist is present, there is no competition for their juveniles. Hence the voracious cannibal can invade as it utilises this unexploited resource. Conversely, when only the cannibals are present, they are unsuccessful in prey capture due to the trade-off of cannibalism. Consequently, there is no serious competition for the prey, which allows the prey specialist to invade. When the same argument applies for certain intermediate types, coexistence is understandable. Admittedly, the trade-off properties complicate the situation, but the idea of the argument remains valid.

Critical function analysis of adaptive dynamics provides a straightforward method for finding evolutionary branching points by tuning local trade-off properties, although additional care is

needed because of simultaneous prey evolution. Coevolution further extends the range of trade-off curvatures that result in evolutionary branching (centre panel of Fig. 5). This is because attainability of the coevolutionary singularity can, to some extent, be maintained by rapid prey evolution when predator evolution tends away from it. Whenever simultaneous prey evolution is necessary to the outcome, the singularity is weakly convergence stable and branching is predicted to be delayed. The findings of Claessen et al. (2007) demonstrated similar delayed evolutionary branching, but with a different underlying mechanism based on demographic stochasticity in small populations. The authors are unaware of any other study with delayed evolutionary branching due to weak convergence stability in a coevolutionary setting.

While critical function analysis is commonly used to find evolutionary branching points, our analysis extends the method for finding evolutionary cycles. Such cycles are genetically driven, and arise through Hopf bifurcation of the canonical Eq. (27). Surprisingly, Hopf bifurcation is equally possible for different types of evolutionary singularities (centre and right panels of Fig. 5). Hopf bifurcation is easily attained by varying either the trade-off curvature or the relative speed between prey and predator evolution. Without coevolution, however, Hopf bifurcation is impossible as the evolutionary dynamics become one-dimensional.

Khibnik and Kondrashov (1997) came up with the idea of constructing evolutionary cycles through Hopf bifurcation of a coupled eco-genetical model, and inverted an example model with such cycles. Their model, however, lacks derivation from individual-level processes, providing no information about the underlying behavioural features that cause the outcome. Genetically driven cycles have also been found using a stochastic simulation model (Dieckmann et al. 1995) and a numerical bifurcation analysis (Dercole et al. 2003). The present work incorporates the idea of Khibnik and Kondrashov into the critical function analysis of adaptive dynamics, resulting in simple conditions for the appearance of a genetically driven evolutionary cycle (Eqs. (52) and (53)). The major advancement is that our approach allows model derivation from individual-level processes with an arbitrary trade-off for the evolving trait. Evolutionary cycles are constructed effortlessly at the very last step of the analysis. Admittedly, these cycles may exist only in a small neighbourhood of the singularity. To find long-term genetic cycles, it is necessary to know how the evolving traits and the ecological environment affect the relative speeds of prey and predator evolution.

Ecogenetically driven cycles involving abrupt attractor switching are easy to understand intuitively, but there is no clear method for finding them. Actual demonstrations are few (Doebeli and Ruxton 1997; Khibnik and Kondrashov 1997; Dercole et al. 2002; Lehtinen and Geritz 2019). Previous demonstrations always involved two catastrophic bifurcations of the ecological environment, each of which caused a switch to the alternative attractor. Besides the present study, we are aware of only one coevolutionary model with these kinds of evolutionary cycles (Khibnik and Kondrashov 1997). The present analysis also demonstrates that, for coevolving species, even just one catastrophic bifurcation is sufficient for the outcome. This occurs when evolutionary trajectories of the resident traits orbit around the generalised Hopf bifurcation of the ecological dynamics (Fig. 7(a)). It appears that as long as ecological bistability is present, many trade-off functions allow the coevolutionary dynamics to involve ecogenetical cycles with two catastrophic bifurcations (subcritical Hopf and fold). Even linear trade-off produces such cycles, suggesting that other demonstrations are easy to find. Furthermore, initially linear trade-off with a steep tail yields a situation, in which attractor switching cycles are the only possible long-term outcome of coevolution (Fig. 7(b)).

In the light of these results, we have reason to expect that many evolutionary predictions are easily overlooked when analysis is restricted to models without ecological bistability. Furthermore, for the same ecological setting, coevolutionary dynamics turn out to be much richer than prey-only evolution (Lehtinen and Geritz 2019). The prevailing view among evolutionary researchers, centred on single-species evolution, needs to be extended to coevolution for a better understanding of the long-term implications for the individual behaviour and the ecological environment.

## Acknowledgements

This research was funded by the Academy of Finland, Centre of Excellence in Analysis and Dynamics Research.

## Appendix A

The outline of the following timescale separation follows that of Lehtinen and Geritz (2019). Here, we extend the model to include several predator types and the trade-off function $\beta(\alpha)$. The full dynamical system before scaling the time and the model parameters is given by

$$\frac{dx_i^F}{dt} = -b_i x_i^F \sum_{j'} y_{j'} + \tfrac{1}{\tau_i} x_i^H - x_i^F \sum_{j'} \beta(\alpha_{j'}) y_{j'}^S + x_i^F G\Big(\sum_{i'} x_{i'}^F\Big) - \mu x_i^F, \tag{A.1}$$

$$\frac{dx_i^H}{dt} = b_i x_i^F \sum_{j'} y_{j'} - \frac{1}{\tau_i} x_i^H - \mu x_i^H, \tag{A.2}$$

$$\frac{dy_j^S}{dt} = -\beta(\alpha_j) y_j^S \sum_{j'} x_{i'}^F + \frac{1}{h} y_j^H - \delta y_j^S + \frac{1}{T} z_j, \tag{A.3}$$

$$\frac{dy_j^H}{dt} = \beta(\alpha_j) y_j^S \sum_{j'} x_{i'}^F - \frac{1}{h} y_j^H - \delta y_j^S, \tag{A.4}$$

$$\frac{dz_j}{dt} = \alpha_j \lambda y_j^S \sum_{j'} z_{j'} + \beta(\alpha_j) \gamma y_j^S \sum_{i'} x_{i'}^F - z_j \sum_{j'} \alpha_{j'} y_{j'}^S - \sigma z_j - \tfrac{1}{T} z_j. \tag{A.5}$$

Let $\varepsilon > 0$, and assume the following scalings for the model parameters: $b = \varepsilon^{-3} b_0$, $\alpha_j = \varepsilon^{-2} \alpha_{j,0}$, $\beta(\alpha) = \varepsilon^{-1} \beta_0(\varepsilon^2 \alpha)$, $\sigma = \varepsilon^{-1} \sigma_0$, $T = \varepsilon^{-1} T_0$, $x_i = \varepsilon^{-1} x_{i,0}$, $y_j = \varepsilon y_{j,0}$, $\tau = \varepsilon^2 \tau_0$, $h = \varepsilon^2 h_0$, and $G(\sum_{i'} x_{i'}^F) = G_0(\varepsilon \sum_{i'} x_{i'}^F)$. Rewriting the above system using these scaled parameters results in

$$\varepsilon^2 \frac{dx_i^F}{dt} = -b_i x_i^F \sum_{j'} y_{j'} + \tfrac{1}{\tau_i} x_i^H - \varepsilon^2 x_i^F \sum_{j'} \beta(\alpha_{j'}) y_{j'}^S + \varepsilon^2 x_i^F G\Big(\sum_{i'} x_{i'}^F\Big) - \varepsilon^2 \mu x_i^F, \tag{A.6}$$

$$\varepsilon^2 \frac{dy_j^S}{dt} = -\beta(\alpha_j) y_j^S \sum_{j'} x_{i'}^F + \frac{1}{h} y_j^H - \varepsilon^2 \delta y_j^S + \frac{\varepsilon^2}{T} z_j, \tag{A.7}$$

$$\varepsilon \frac{dz_j}{dt} = \alpha_j \lambda y_j^S \sum_{j'} z_{j'} + \beta(\alpha_j) \gamma y_j^S \sum_{i'} x_{i'}^F - z_j \sum_{j'} \alpha_{j'} y_{j'}^S - \sigma z_j - \tfrac{1}{\varepsilon^2} z_j, \tag{A.8}$$

$$\frac{dx_i}{dt} = x_i^F G\Big(\sum_{i'} x_{i'}^F\Big) - \mu x_i - x_i^F \sum_{j'} \beta(\alpha_{j'}) y_{j'}^S, \tag{A.9}$$

$$\frac{dy_j}{dt} = \frac{1}{T} z_j - \delta y_j. \tag{A.10}$$

Here, for convenience, we dropped the subindex zero from the scaled parameters, and replaced the equations for hiding prey, $x_i^H$, and handling predators, $y_j^H$, with their respective total population numbers $x_i$ and $y_j$. To investigate the above dynamics on different timescales, we introduce scaled times $t^{**} := \varepsilon^{-2}t$ and $t^* := \varepsilon^{-1}t$. The short timescale dynamics is obtained by rewriting the system in terms of $t^{**}$, and then letting $\varepsilon \to 0$ results in

$$\frac{dx_i^F}{dt^{**}} = -b_i x_i^F \sum_{j'} y_{j'} + \frac{1}{\tau_i} x_i^H, \tag{A.11}$$

$$\frac{dy_j^S}{dt^{**}} = -\beta(\alpha_j) y_j^S \sum_{i'} x_{i'}^F + \frac{1}{h} y_j^H, \tag{A.12}$$

which are equivalent to (3) and (4), and where the variables $x$, $y$, and $z$ are constants. On this timescale, the population numbers for $x_i^F$ and $y_j^S$ attain quasi-steady states (5) and (6), respectively. Then, the intermediate timescale dynamics is obtained by rewriting the full system in terms of $t^*$ and the quasi-steady states, and then letting $\varepsilon \to 0$ results in

$$\frac{dz_j}{dt^*} = \alpha_j \lambda y_j^S \sum_{j'} z_{j'} + \beta(\alpha_j)\gamma y_j^S \sum_{i'} x_{i'}^F - z_j \sum_{j'} \alpha_{j'} y_{j'}^S - \sigma z_j, \tag{A.13}$$

which is equivalent to (7), and where $x_i$ and $y_j$ are constants.

## References


Abrams, P.A., 1986. Adaptive responses of predators to prey and prey to predators: the failure of the arms-race analogy. Evolution 40 (6), 1229–1247. doi:10.1111/j.1558-5646.1986.tb05747.x.

Abrams, P.A., 1990. The evolution of anti-predator traits in prey in response to evolutionary change in predators. Oikos 59 (2), 147–156. doi:10.2307/3545529.

Abrams, P.A., 2000. The evolution of predator-prey interactions: theory and evidence. Annu. Rev. Ecol. Syst. 31, 79–105. doi:10.1146/annurev.ecolsys.31.1.79.

Abrams, P.A., Matsuda, H., 1993. Effects of adaptive predatory and anti-predator behaviour in a two-prey-one-predator system. Evolut. Ecol. 7 (3), 312–326. doi:10.1007/BF01237749.

Abrams, P.A., Matsuda, H., 1997. Fitness minimization and dynamic instability as a consequence of predator-prey coevolution. Evolut. Ecol. 11 (1), 1–20. doi:10.1023/A:1018445517101.

Beddington, J.R., 1975. Mutual interference between parasites or predators and its effect on searching efficiency. J. Animal Ecol. 44 (1), 331–340. doi:10.2307/3866.

van den Bosch, F., de Roos, A.M., Gabriel, W., 1988. Cannibalism as a life boat mechanism. J. Math. Biol. 26, 619–633. doi:10.1007/BF00276144.

Bowers, R.G., Hoyle, A., White, A., Boots, M., 2005. The geometric theory of adaptive evolution: trade-off and invasion plots. J. Theor. Biol. 233 (3), 363–377. doi:10.1016/j.jtbi.2004.10.017.

Brown, J.S., Vincent, T.L., 1992. Organization of predator-prey communities as an evolutionary game. Evolution 46 (5), 1269–1283. doi:10.1111/j.1558-5646.1992.tb01123.x.

Champagnat, N., Ferrière, R., Ben Arous, G., 2001. The canonical equation of adaptive dynamics: a mathematical view. Selection 2, 73–83. doi:10.1556/Select.2.2001.1-2.6.

Claessen, D., Andersson, J., Persson, L., de Roos, A.M., 2007. Delayed evolutionary branching in small populations. Evolutionary Ecology Research 9, 51–69.

Claessen, D., de Roos, A.M., Persson, L., 2000. Dwarfs and giants: cannibalism and competition in size-structured populations. The American Naturalist 155 (2), 219–237. doi:10.1086/303315.

Dawkins, R., Krebs, J.R., 1979. Arms races between and within species. Proc. R. Soc. B 205 (1161), 489–511. doi:10.1098/rspb.1979.0081.

DeAngelis, D.L., Goldstein, R.A., O'Neill, R.V., 1975. A model for trophic interaction. Ecology 56 (4), 881–892. doi:10.2307/1936298.

Dercole, F., 2003. Remarks on branching-extinction evolutionary cycles. J. Math. Biol. 47 (6), 569–580. doi:10.1007/s00285-003-0236-4.

Dercole, F., Ferrière, R., Rinaldi, S., 2002. Ecological bistability and evolutionary reversals under asymmetrical competition. Evolution 56 (6), 1081–1090. doi:10.1111/j.0014-3820.2002.tb01422.x.

Dercole, F., Irisson, J.O., Rinaldi, S., 2003. Bifurcation analysis of a prey-predator coevolution model. SIAM J. Appl. Math. 64 (4), 1378–1391. doi:10.1137/S0036139902411612.

Dercole, F., Rinaldi, S., 2002. Evolution of cannibalistic traits: scenarios derived from adaptive dynamics. Theor. Populat. Biol. 62 (4), 365–374. doi:10.1016/S0040-5809(02)00008-4.

Dieckmann, U., Law, R., 1996. The dynamical theory of coevolution: a derivation from stochastic ecological processes. J. Math. Biol. 34 (5–6), 579–612. doi:10.1007/BF02409751.

Dieckmann, U., Marrow, P., Law, R., 1995. Evolutionary cycling in predator-prey interactions: population dynamics and the Red Queen. J. Theor. Biol. 176 (1), 91–102. doi:10.1006/jtbi.1995.0179.

Doebeli, M., Ruxton, G.D., 1997. Evolution of dispersal rates in metapopulation models: branching and cyclic dynamics in phenotype space. Evolution 51 (6), 1730–1741. doi:10.2307/2410996.

Downes, S., Shine, R., 1998. Sedentary snakes and gullible geckos: predator-prey coevolution in nocturnal rock-dwelling reptiles. Anim. Behav. 55, 1373–1385. doi:10.1006/anbe.1997.0704.

Edgar, W.D., 1969. Prey and predators of the wolf spider Lycosa lugubris. J. Zool. 159 (4), 405–411. doi:10.1111/j.1469-7998.1969.tb03897.x.

Fox, L.R., 1975. Cannibalism in natural populations. Annu. Rev. Ecol. Syst. 6 (1), 87–106. doi:10.1146/annurev.es.06.110175.000511.

Geritz, S.A.H., Gyllenberg, M., 2012. A mechanistic derivation of the DeAngelis-Beddington functional response. J. Theor. Biol. 314, 106–108. doi:10.1016/j.jtbi.2012.08.030.

Geritz, S.A.H., Gyllenberg, M., 2014. The DeAngelis-Beddington functional response and the evolution of timidity of the prey. J. Theor. Biol. 359, 37–44. doi:10.1016/j.jtbi.2014.05.015.

Geritz, S.A.H., Gyllenberg, M., Jacobs, F.J.A., Parvinen, K., 2002. Invasion dynamics and attractor inheritance. J. Math. Biol. 44 (6), 548–560. doi:10.1007/s002850100136.

Geritz, S.A.H., Kisdi, E., Meszéna, G., Metz, J.A.J., 1998. Evolutionarily singular strategies and the adaptive growth and branching of the evolutionary tree. Evolut. Ecol. 12 (1), 35–57. doi:10.1023/A:1006554906681.

Geritz, S.A.H., Kisdi, E., Yan, P., 2007. Evolutionary branching and long-term coexistence of cycling predators: critical function analysis. Theor. Populat. Biol. 71, 424–435. doi:10.1016/j.tpb.2007.03.006.

Geritz, S.A.H., Metz, J.A.J., Kisdi, E., Meszéna, G., 1997. Dynamics of adaptation and evolutionary branching. Phys. Rev. Lett. 78 (10), 2024–2027. doi:10.1103/PhysRevLett.78.2024.

Getto, P.H., Diekmann, O., de Roos, A.M., 2005. On the (dis) advantages of cannibalism. Journal of Mathematical Biology 51, 695–712. doi:10.1007/s00285-005-0342-6.

Goodall, J., 1977. Infant killing and cannibalism in free-living chimpanzees. Folia Primatologica 28 (4), 259–282. doi:10.1159/000155817.

Heiling, A.M., Herberstein, M.E., 2004. Predator-prey coevolution: Australian native bees avoid their spider predators. Proc. R. Soc. B 271, S196–S198. doi:10.1098/rsbl.2003.0138.

Holt, R.D., 1977. Predation, apparent competition, and the structure of prey communities. Theor. Populat. Biol. 12 (2), 197–229. doi:10.1016/0040-5809(77)90042-9.

Hrdy, S.B., 1979. Infanticide among animals: a review, classification, and examination of the implications for the reproductive strategies of females. Ethol. Sociobiol. 1 (1), 13–40. doi:10.1016/0162-3095(79)90004-9.

Khibnik, A.I., Kondrashov, A.S., 1997. Three mechanisms of Red Queen dynamics. Proc. R. Soc. B 264 (1384), 1049–1056. doi:10.1098/rspb.1997.0145.

Kisdi, E., 2006. Trade-off geometries and the adaptive dynamics of two co-evolving species. Evolut. Ecol. Res. 8 (6), 959–973.

Kisdi, E., Jacobs, F.J.A., Geritz, S.A.H., 2001. Red Queen evolution by cycles of evolutionary branching and extinction. Selection 2 (1), 161–176. doi:10.1556/Select.2.2001.1-2.12.

Kohmatsu, Y., Nakano, S., Yamamura, N., 2001. Effects of head shape variation on growth, metamorphosis and survivorship in larval salamanders (Hynobius retardatus). Ecol. Res. 16 (1), 73–83. doi:10.1046/j.1440-1703.2001.00373.x.

Lawton, J.H., 1970. Feeding and food energy assimilation in larvae of the damselfly Pyrrhosoma nymphula (Sulz.) (Odonata: Zygoptera). J. Anima. Ecol. 39 (3), 669–689. doi:10.2307/2859.

Lehtinen, S.O., Geritz, S.A.H., 2019. Cyclic prey evolution with cannibalistic predators. J. Theor. Biol. 479, 1–13. doi:10.1016/j.jtbi.2019.06.025.

Leimar, O., 2009. Multidimensional convergence stability. Evolut. Ecol. Res. 11, 191–208.

Lima, S.L., Dill, L.M., 1990. Behavioral decisions made under the risk of predation: a review and prospectus. Canad. J. Zool. 68 (4), 619–640. doi:10.1139/z90-092.

MacArthur, R.H., Levins, R., 1964. Competition, habitat selection, and character displacement in a patchy environment. Proc. Natl. Acad. Sci. U.S.A. 51 (6), 1207–1210. doi:10.1073/pnas.51.6.1207.

Marrow, P., Dieckmann, U., Law, R., 1996. Evolutionary dynamics of predator-prey systems: an ecological perspective. J. Math. Biol. 34 (5–6), 556–578. doi:10.1007/s002850050021.

Marrow, P., Law, R., Cannings, C., 1992. The coevolution of predator-prey interactions: ESSs and Red Queen dynamics. Proc. R. Soc. B: Biological Sciences 250 (1328), 133–141. doi:10.1098/rspb.1992.0141.

Maynard Smith, J., 1982. Evolution and the Theory of Games. Cambridge University Press, Cambridge doi:10.2277/0521288843.

Maynard Smith, J., Price, G.R., 1973. The logic of animal conflict. Nature 246, 15–18. doi:10.1038/246015a0.

de Mazancourt, C., Dieckmann, U., 2004. Trade-off geometries and frequency-dependent selection. Am. Naturalist 164 (6), 765–778. doi:10.1086/424762.

Polis, G.A., 1981. The evolution and dynamics of intraspecific predation. Annu. Rev. Ecol. Syst. 12, 225–251. doi:10.1146/annurev.es.12.110181.001301.

Popova, O.A., Sytina, L.A., 1977. Food and feeding relations of Eurasian perch (Perca fluviatilis) and pikeperch (Stizostedion lucioperca) in various waters of the USSR. J. Fisher. Res. Board Canada 34 (10), 1559–1570. doi:10.1139/f77-219.

Rosenzweig, M.L., 1973. Evolution of the predator isocline. Evolution 27 (1), 84–94. doi:10.2307/2407121.

Rosenzweig, M.L., MacArthur, R.H., 1963. Graphical representation and stability conditions of predator-prey interactions. Am. Natur. 97 (895), 209–223. doi:10.1086/282272.

Stenseth, N.C., 1985. On the evolution of cannibalism. J. Theor. Biol. 115 (2), 161–177. doi:10.1016/S0022-5193(85)80093-X.

Van Valen, L., 1973. A new evolutionary law. Evolut. Theory 1, 1–30.

Wakano, J.Y., Kohmatsu, Y., Yamamura, N., 2002. Evolutionary dynamics of frequency-dependent growth strategy in cannibalistic amphibians. Evolut. Ecol. Res. 4, 719–736.

West, K., Cohen, A., Baron, M., 1991. Morphology and behavior of crabs and gastropods from lake Tanganyika, Africa: implications for lacustrine predator-prey coevolution. Evolution 45 (3), 589–607. doi:10.2307/2409913.